Tailoring the biofunctionality of collagen biomaterials via tropoelastin incorporation and EDC-crosslinking

Daniel V. Bax[1,2*], Malavika Nair[1], Anthony S. Weiss[3,4,5], Richard W. Farndale[2], Serena M. Best[1], Ruth E. Cameron[1]

[1] Department of Materials Science and Metallurgy, University of Cambridge, 27 Charles Babbage Road, Cambridge, CB3 0FS, United Kingdom

[2] Department of Biochemistry, University of Cambridge, Downing Site, Cambridge, CB2 1QW, United Kingdom

[3] Life and Environmental Sciences, University of Sydney, NSW, 2006, Australia

[4] Charles Perkins Centre, University of Sydney, NSW, 2006, Australia

[5] Sydney Nano Institute, University of Sydney, NSW, 2006, Australia

*Corresponding author Tel.: +44 1223 334560; fax: +44 1223 334567.

E-mail address: dvb24@cam.ac.uk

Keywords: collagen, tropoelastin, cellular response

Graphical Abstract

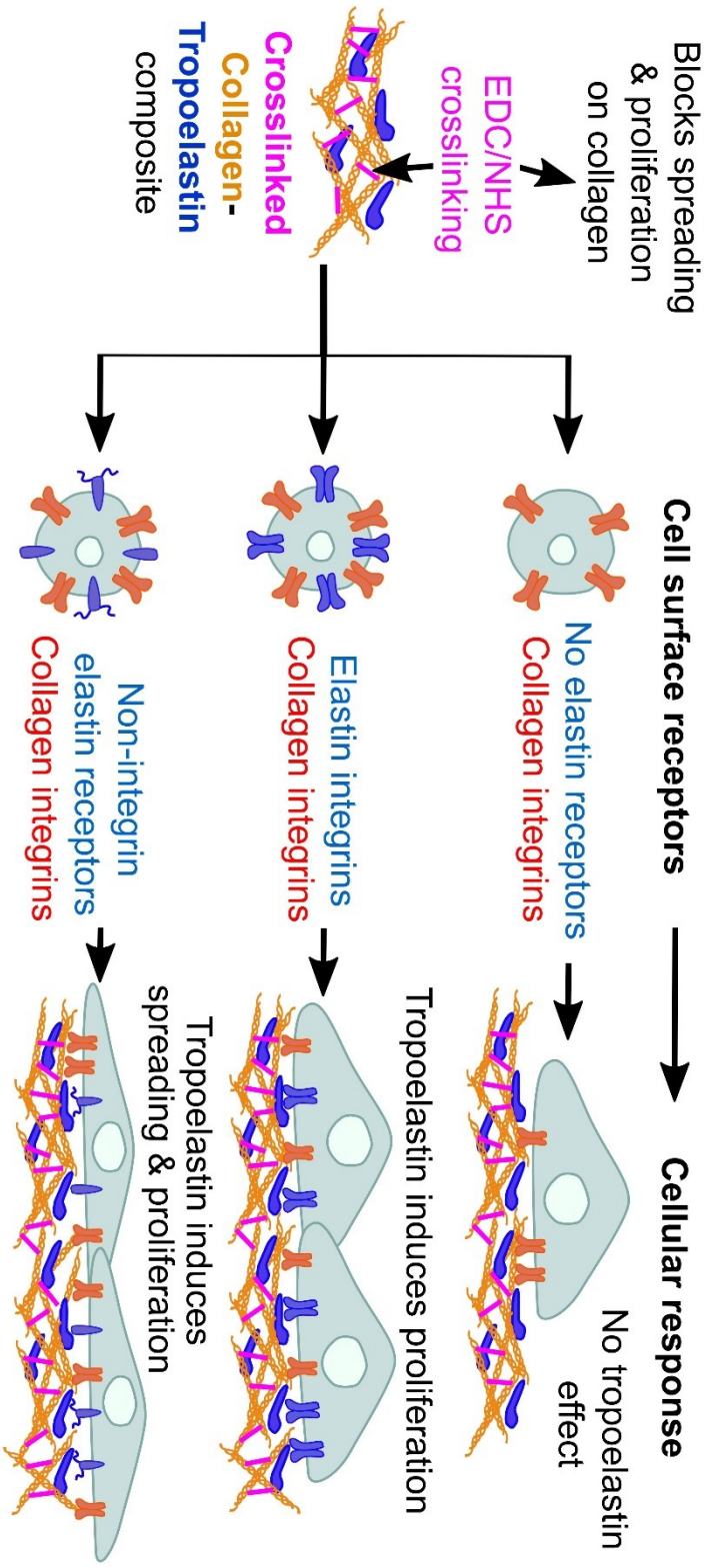

1. Abstract

Recreating the cell niche of virtually all tissues requires composite materials fabricated from multiple extracellular matrix (ECM) macromolecules. Due to their wide tissue distribution, physical attributes and purity, collagen, and more recently, tropoelastin, represent two appealing ECM components for biomaterials development. Here we blend tropoelastin and collagen, harnessing the cell-modulatory properties of each biomolecule. Tropoelastin was stably co-blended into collagen biomaterials and was retained after EDC-crosslinking. We found that human dermal fibroblasts (HDF), rat glial cells (Rugli) and HT1080 fibrosarcoma cells ligate to tropoelastin via EDTA-sensitive and EDTA-insensitive receptors or do not ligate with tropoelastin, respectively. These differing elastin-binding properties allowed us to probe the cellular response to the tropoelastin-collagen composites assigning specific bioactivity to the collagen and tropoelastin component of the composite material. Tropoelastin addition to collagen increased total Rugli cell adhesion, spreading and proliferation. This persisted with EDC-crosslinking of the tropoelastin-collagen composite. Tropoelastin addition did not affect total HDF and HT1080 cell adhesion; however, it increased the contribution of cation-independent adhesion, without affecting the cell morphology or, for HT1080 cells, proliferation. Instead, EDC-crosslinking dictated the HDF and HT1080 cellular response. These data show that a tropoelastin component dominates the response of cells that possess non-integrin based tropoelastin receptors. EDC modification of the collagen component directs cell function when non-integrin tropoelastin receptors are not crucial for cell activity. Using this approach, we have assigned the biological contribution of each component of tropoelastin-collagen composites, allowing informed biomaterial design for directed cell function via more physiologically relevant mechanisms.

2. Introduction

It is critically important that biomaterials for tissue engineering applications elicit an appropriate cellular response. In their native setting, cells are surrounded by the Extracellular Matrix (ECM), which provides physical and biochemical cues for tissue development [1]. As such, ECM macromolecules are frequently used for biomaterials fabrication, thereby harnessing their natural cell-guiding capacity. These ECM macromolecules include structural ECM components such as collagens, elastin, fibronectin and laminins [2], matricellular molecules such as thrombospondin-1 and tenascin-C [3] and glycosaminoglycans such as hyaluronan and chondroitin sulfate [4]. Of these, collagen I is the most frequently used ECM macromolecule for biomaterial applications. This is due to its abundance in native tissue, physical strength and stiffness, biocompatibility, purity and cost [1,5]. Despite these beneficial attributes, it is doubtful that materials fabricated solely from collagen, and so representing only one of a complex array of the cell-binding macromolecules found in the cell niche, can adequately recapitulate the complexity of cell signals derived from the native ECM. To address this deficit, here we have examined tropoelastin incorporation into collagen biomaterials, and have delineated the effect that this bestows upon cells containing differing elastin-binding receptors. This includes comparison of Rugli cells which are more responsive to soluble elastin against HT1080 cells which are relatively insensitive to elastin [6]. In doing so we show that tropoelastin-collagen biomaterials can selectively support the bioactivity of specific cell types, depending on their tropoelastin-receptor usage. This aids exploitation of the beneficial attributes of tropoelastin such as guiding mesenchymal stem cell (MSC) phenotype, control of vascular smooth muscle cell proliferation and non-thrombogenicity in a collagen-based biomaterial.

Elastic fibres, composed predominantly from crosslinked elastin monomers, are a major constituent of a wide range of elastic tissues, for example accounting for up to 50% of arterial wall dry mass [7]. Unlike collagen, which provides resilience [8], elastic fibres are crucial for the elastic recoil of tissues [9]. These elastic fibres are deposited by cells as the monomeric elastin precursor, tropoelastin. In turn, cell ligating sequences on tropoelastin have been shown to influence cell adhesion, spreading, proliferation and MSC phenotypic responses [10–12]. When utilised as a biomaterial, the cell-biological properties of elastin are frequently attributed to the elasticity and roughness of the substrate, however recent evidence shows direct receptor-mediated effects on MSCs which are not mechanotransducive [11]. Instead this occurs through tropoelastin receptors including the elastin binding protein (EBP)[13,14], cell surface heparan and chondroitin sulfate-containing glycosaminoglycans [15] and integrins [16–19]. These differ markedly from collagen receptors such as integrins $\alpha_1\beta_1$, $\alpha_2\beta_1$, $\alpha_{10}\beta_1$, and $\alpha_{11}\beta_1$ [20], Discoidin Domain Receptors (DDR) and the secreted protein acidic and rich in cysteine (SPARC)[21]. As elastin can activate different cellular receptors than collagen, it has been proposed that addition of elastin to collagen biomaterials could tailor cell-receptor engagement and hence the cellular response to the composite material [6]. Therefore, we have examined the combination of tropoelastin and collagen to exploit these recently described mitogenic and cell attractive properties of tropoelastin. Elastin, in a number of different forms, has been employed for biomaterial fabrication, including soluble (SE) and insoluble (IE) elastin, tropoelastin (TE) and synthetic elastin-like polypeptides [22]. Of these, tropoelastin was chosen here as its cell-binding regions are inherent accessible, some of which may be inaccessible in SE or IE [23]. Elastin-like polypeptides were excluded here as they do not contain the full complement of cell ligating sequences found in tropoelastin. Although elastin interacts favourably with a wide range of cell types, and has non-thrombogenic potential [24], in isolation it, too, does not fully replicate the complexity of

the native ECM. As such, elastin has been integrated into collagen biomaterials to combine the beneficial attributes of each ECM component [25]. Previously, elastin addition has been shown to reduce the tensile and compressive modulus compared to collagen-only materials [26]. However, the effect of elastin addition on cellular behaviour appears more nuanced, with some studies showing increased fibroblast proliferation [27], others little effect [28,29], and yet others decreased cellular proliferation [30–33] compared to collagen-only materials. This divergence of cell behaviour is presumably due to the differing elastin forms, cell types and experimental protocols employed by each study. Direct comparison between an elastin-ligating and elastin-insensitive cell line showed that IE and SE addition to collagen could alter the cell response via 2 mechanisms; 1) direct cell receptor engagement by elastin and 2) indirectly, presumably via alterations in the material stiffness or modulation of cell ligation with the collagen component of the composite [6]. Despite this, the cell-biological effect of tropoelastin addition to collagen biomaterials is unknown. Here, 2-dimensional composite tropoelastin-collagen films were studied to examine the role of receptor engagement while excluding compounding variables, for example geometry, diffusion, and porosity, that are present in 3-dimenstional systems. In effect these mimic the pore wall of a 3-dimensional system.

Collagen biomaterials possess many useful physical attributes; however, crosslinking is required for material integrity, particularly under aqueous and enzymatic conditions [34]. Of the many physical and chemical crosslinkers studied [35], 1-ethyl-3-(3-dimethylaminopropyl-carbodiimide hydrochloride (EDC) in the presence of N-hydroxy-succinimide (NHS) is attractive. This is due to the formation of zero-length amide bonds, ability to tailor the mechanical and degradation properties of the material [36], and easy removal of cytotoxic reagents and products using a simple washing regime [37]. To optimise bond formation, and so physical integrity, a ratio of 5EDC:2NHS:1COOH group on collagen in a 75% ethanol

solution is frequently used [36]. EDC bonds carboxylic acid containing (aspartic acid and glutamic acid) amino acid side chains to adjacent primary amine containing (lysine) side chains. This is important as the consensus Gxx′GEx″ (single amino acid code) integrin-binding sequence in collagen contains a critically required carboxylic acid group on the glutamic acid (E) side chain [38]. Therefore, crosslinking with EDC can ablate native integrin-mediated cell adhesion, presumably through EDC modification of this glutamic acid side chain [39]. Intriguingly, native cell adhesion on EDC-crosslinked collagen is replaced by non-native interactions that are not sensitive to divalent cation chelation with Ethylenediaminetetraacetic acid (EDTA) and do not support cell proliferation [39]. As such, careful control over the EDC-crosslinking conditions is required to retain sufficient cell-binding sequences for appropriate cell engagement to collagen biomaterials.

We have previously noted that IE or SE addition to collagen biomaterials can alter the cell response when crosslinked with a single EDC condition of 5EDC:2NHS:1COOH group on collagen [6]. As these IE and SE additions are bulky and have been crosslinked *in vivo* prior to their extraction, they alter multiple material attributes simultaneously [6,29]. By contrast, tropoelastin has a mass of ~60 kDa [40], self-associates by coacervation [41] and has well studied cell-binding characteristics [13–19]. The aim of this study was to investigate tropoelastin addition to collagen biomaterials as it represents the non-crosslinked, monomeric precursor of elastin fibres. We postulate that tropoelastin addition can provide both adhesive and mitogenic capacity to collagen biomaterials. This composite was crosslinked with varying degrees of EDC-crosslinking as the interaction between collagen, tropoelastin and EDC-crosslinking is not known. In particular, the influence of EDC crosslinking on bioactivity is fundamentally important for their utility as biomaterials. Three different model cell lines, Rugli, HT1080 and human dermal fibroblasts, each with distinct elastin-receptor usage, were used to probe the relationship between tropoelastin addition, EDC-crosslinking

and cellular behaviour. This methodical approach has allowed us to show the importance of elastin addition and collagen-crosslinking on the cell-biological response to tropoelastin-collagen composite biomaterials. In doing so we can combine the recently described cell-modulatory capacity of tropoelastin with the well-established biophysical properties of EDC-crosslinked collagen biomaterials, with potential for elastic tissue replacement, *in vitro* cell expansion and *in vitro* cell culture platforms.

3. Materials and Methods

3.1. *Materials*

Unless stated otherwise all reagents were purchased from Sigma Aldrich, UK. 4% v/v acetic acid was purchased from Alfa Aesar, U.S. Recombinant human tropoelastin corresponding to amino acid residues 27–724 of GenBank entry AAC98394 (gi 182020) was purified as previously described [42].

3.2. *Sample preparation*

1 wt% suspensions of insoluble bovine dermal collagen (Devro, UK), were swollen in 0.05 M acetic acid overnight at 4 °C. These were homogenised in a pre-chilled blender then centrifuged for 2 min at 2500 rpm in a Hermle Z300 (Labortechnik, Germany) centrifuge to remove air bubbles. Recombinant human tropoelastin, prepared as in [42], was solubilised to 1 mg/mL in 0.05 M acetic acid. Tropoelastin was incorporated via 3 different approaches as detailed in table 1.

3.3. *Tropoelastin detection*

Films were blocked with 400 µL of blocking buffer (2% (w/v) bovine serum albumin (BSA), 0.1% (v/v) Tween-20 in phosphate buffered saline (PBS)) for 1 h at room temperature then washed 3 times 400 µL wash buffer (0.1% (w/v) BSA, 0.1% (v/v) Tween-20 in PBS). Tropoelastin was detected with 300 µL of 1:2000 diluted mouse anti-elastin antibody (clone BA-4) in wash buffer for 1 h at room temperature. The samples were washed in 3 times 400 µL wash buffer before incubation in 300 µL of either 1:10000 diluted goat anti-mouse IgG-HRP conjugated secondary antibody (DAKO, Agilent, U.S.) in wash buffer for Enzyme Linked Immunosorbent Assays (ELISA) or 1:1000 diluted goat anti-mouse-FITC conjugated

secondary antibody for fluorescence microscopy. After incubation for 45 min at room temperature the secondary antibody was removed, and the samples washed 4 times in 400 µL wash buffer for 20 min each wash. For ELISA analysis 400 µL of TMB solution (Thermo, U.S.) was added for 20 min at room temperature then the absorbance was read at 370 nm (A_{652}) on a SPECTROstar Nano plate reader (BMG Labtech, Germany). For fluorescent microscopy (Ex. 450-490 nm, Em. 500-550 nm) the samples were mounted onto a slide in a Zeiss Observer Z1 fluorescent microscope fitted with an Axiocam 503 camera (Zeiss, Germany). The fluorescent intensity was measured using ImageJ (NIH, U.S.).

3.4. *Atomic Force Microscopy (AFM)*

Films on 1 cm^2 microscope glass slides were characterised using peak force quantitative nanomechanical mapping (QNM). 5 µm x 5 µm (Peak Force Mode) or 500 nm x 500 nm (Tapping Mode) regions of the films were imaged using an atomic force microscope (Multimode 8, Bruker, U.S.) using a single tip (Tap300 Al-G, Budget Sensors, Bulgaria). A sapphire substrate was used to calibrate the deflection sensitivity of the tip, and a PS-LDPE standard was used to set the QNM parameters. Gain, scan rate and set point were automatically set by Nanoscope ScanAsyst. The raw AFM data channels were processed for scanner drift artefact removal (align rows and horizontal scar removal), the channel minima were set to zero to facilitate comparison across samples and the data were flattened using a polynomial background removal tool using Gwyddion and its *pygwy* batch processing module. The results show representative micrographs of the topography and deformation channels of films.

3.5. *Primary amine content analysis*

To determine the free amine content, 200 µL of Ninhydrin solution (0.25 g ninhydrin in 5 mL ethanol) was added to each well, sealed with Parafilm and incubated at 80 °C for 20 min. After cooling to room temperature, 250 µL of 50% (v/v) isopropanol was added. 200 µL of the reaction volume was transferred to a 96 well plate and the absorbance measured at 570 nm on a SPECTROstar Nano plate reader (BMG Labtech, Germany).

3.6. *Cell culture*

HT1080 human fibrosarcoma cells and human dermal fibroblasts (HDF) were obtained from the European Collection of Animal Cell Cultures, Porton Down, UK. Rugli rat glioma cells were from Dr. J. Gavrilovic, University of East Anglia, UK. All cell lines were cultured on tissue culture plastic flasks maintained in a humidified incubator with 5% CO_2 at 37 °C in Dulbecco's modified Eagle's medium (DMEM) containing 10% (v/v) fetal bovine serum and 1% (v/v) streptomycin/penicillin (complete media). Once 70-80% confluent the cells were detaching from the cell culture flasks with 0.05% (w/v) trypsin / 0.02% (w/v) EDTA and re-suspended at a ratio of 1:10 for HT1080 cells, 1:20 for Rugli cells and 1:3 for HDFs.

3.7. *Cell adhesion analysis*

To analyse direct cell attachment to tropoelastin, 48-well tissue culture plates were coated with either tropoelastin diluted from a 1 mg/mL stock solution in PBS or with 5 µg/mL of soluble collagen I (First Link (UK) Ltd.). For collagen-tropoelastin films the wells were washed once with PBS to hydrate the film. For both analyses the wells were aspirated and non-specific cell binding blocked with 400 µL of 2% (w/v) BSA in PBS for 1 h at room temperature. The wells were washed 3 times with PBS then 200 µL of cells were seeded at a density of $2x10^5$ cells/mL in DMEM (serum-free). For inhibition assays, EDTA (final

concentration 5 mM), α-lactose (final concentration 10 mM), and/or heparan sulfate (final concentration 10 μg/mL) in DMEM were added to each well. The volume in each well was made up to 100 μL with DMEM then 100 μL of cells was added to achieve a final density $2x10^5$ cell/mL. After incubation for 1 h at 37 °C/5% CO_2 loosely adherent cells were removed with 3 times 400 μL PBS washes, and then the cells were lysed in 100 μL of lysis buffer (2% (v/v) TritonX-100 in water) for 2 h at room temperature. The cells were detected by adding 100 μL of LDH substrate (Sigma Aldrich, UK) for 20 min at room temperature, then the absorbance measured at 490nm (A_{490}) on a SPECTROstar Nano plate reader (BMG Labtech, Germany).

3.8. *Cell spreading analysis*

Collagen-tropoelastin films and 5 μg/mL soluble collagen coated tissue culture plastic were prepared and BSA-blocked as for adhesion analysis. 200 μL of cells at a density of $1x10^5$ cells/mL in DMEM (serum-free) were seeded and incubated at 37 °C/5% CO_2 for 120 min. 50 μL of glutaraldehyde (25% (w/v)) was added directly to the cell media to achieve a final concentration of 5% (w/v). After incubating at room temperature for 20 min the samples were washed 3 times 400 μL PBS, permeabilised with 200 μL of 0.5% (w/v) Triton X-100 in PBS for 5 min at room temperature, then washed 3 times 400 μL PBS. The samples were blocked with blocking buffer for 1 h at room temperature, stained with 200 μL of 0.01% (w/v) rhodamine phalloidin (Molecular Probes, U.S., made up to manufacturer's instructions) for 30 min at room temperature in the dark, then washed 3 times 400 μL PBS. The cell nuclei were stained with 200 μL of 3.5 μM DAPI in H_2O for 2 min then washed extensively with H_2O. The samples were visualised using a 20x magnification objective lens on a Zeiss Observer Z1 fluorescent microscope fitted with an Axiocam 503 camera. The cell area was calculated from 6 representative images by measuring the cell-derived area of rhodamine-

phalloidin stained images in ImageJ. The cell number for each image was calculated from DAPI stained images by using the nucleus counter plug-in feature of ImageJ. The average cell area was calculated:

$$Cell\,area = \frac{Total\,cell\,area \in an\,image}{Cell\,count \in an\,image}$$

3.9. *Cell growth*

Samples were prepared and BSA-blocked as for spreading analysis except that all solutions were filter-sterilised. 200 µL of cells were seeded at a density of $1x10^5$ cells/mL in complete media and incubated at 37 °C/5% CO_2 for 2 h (day 0), 3 or 5 days. At each time point the cells were fixed, permeabilised, blocked and DAPI stained as for spreading analysis. The cell nuclei were visualised using a 10x objective lens on a Zeiss Observer Z1 fluorescent microscope fitted with an Axiocam 503 camera and the cell nuclei counted as for spreading analysis. Values represent means of 6 measurements.

3.10. *Statistical analysis*

Unless otherwise stated all error bars indicate standard deviations from the mean. Statistical significance was determined with a student t-test with unequal variance (Excel). Multiple *p* values show the degree of confidence, where N/S indicates >0.05, * indicates $p \leq 0.05$, ** indicates $p \leq 0.01$, *** indicates $p \leq 0.001$ and **** indicates $p \leq 0.0001$.

4. Results

4.1. *Tropoelastin-collagen composite fabrication.*

Several strategies were tested for incorporating tropoelastin into collagen-based materials. These included physisorption, air drying, adsorption during EDC crosslinking and co-blending. ELISA analysis showed that tropoelastin could adsorb onto the surface of a pre-cast collagen film (Figure 1A). The amount of bound tropoelastin increased linearly with coating concentrations up to 5 μg/mL. A smaller increase in bound tropoelastin was observed with coating concentrations up to 50 μg/mL. Although tropoelastin can adsorb onto collagen films, this surface bound tropoelastin was lost upon NHS/EDC crosslinking (Figure 1B). Similarly, no tropoelastin was detected after NHS/EDC crosslinking of tropoelastin that had been air-dried onto the collagen film (Supplementary Fig 1A) or tropoelastin that was included during the EDC/NHS crosslinking procedure (Supplementary Fig 1B). The loss of surface-bound tropoelastin was observed for the 0% NHS/EDC (i.e. solvent only) condition.

As immersion in ethanol removes surface immobilised tropoelastin, we instead combined tropoelastin into the collagen slurry during film fabrication. ELISA detection of tropoelastin incorporated via this blending approach (Figure 1C) was linearly dependent upon the proportion (presented as a % of the collagen mass) of tropoelastin included into the collagen slurry. The amount of tropoelastin present after 100% NHS/EDC crosslinking was only slightly lower than for non-crosslinked controls, indicating that only a small proportion of the tropoelastin was being lost to the ethanol solvent during crosslinking. A small degree of non-linear detection was noted with 10% and 20% (w/w) tropoelastin inclusion which could be due to saturation of the HRP enzyme detection in the ELISA assay. Therefore, the tropoelastin content was confirmed by fluorescent intensity measurements using a FITC-conjugated secondary antibody (Figure 1D). This showed a very similar trend to ELISA

detection. A slight increase in fluorescence intensity was observed for the no primary antibody control, presumably due to tropoelastin autofluorescence [43]. Fluorescent microscopy images (Figure 1E) indicate a homogeneous tropoelastin distribution in the inter-collagen fibre spaces. The no primary antibody controls showed a low level of fluorescence compared to BA-4 antibody detection (Figure 1E). The tropoelastin content was limited to 20% because films containing 40% tropoelastin were not stable under long-term cell culture, undergoing buckling and deformation [data not shown]. AFM topography measurements (Figure 2) show that at the micron length scale, the surface topography was not altered by the addition of tropoelastin. The non-crosslinked films displayed a matrix of low homogenous deformation (and therefore high stiffness) with small spherical domains of high deformation. In crosslinked films, the areas of higher deformation were more finely and evenly dispersed across the sample surface. At the highest concentrations of tropoelastin (10% and 20%), filaments of high deformation (white/light green) can be seen embedded within the stiffer matrix (dark green). The median deformation or strain experienced by the surface increased with tropoelastin addition for both crosslinked and non-crosslinked samples, with a more pronounced effect observed for the 100% EDC crosslinked samples. (Supplementary Figure 2A). At higher magnification (Supplementary Figure 3), 0.5% (w/w) tropoelastin addition had no effect on the surface topography, with no effect on the root mean square (RMS) roughness of the films (Supplementary Figure 2B). With between 1% and 10% (w/w) tropoelastin addition, a filamentous topology was observed. A relatively amorphous surface topography was observed at 20% (w/w) tropoelastin content. Ninhydrin detection showed that inclusion of increasing tropoelastin content did not alter the number of free amine groups (Supplementary Figure 4A). Instead, the number of free amine groups was dependent upon the degree of EDC-crosslinking (Supplementary Figure 4B).

4.2. *Cell adhesion to tropoelastin.*

Three cell lines were chosen to evaluate the cell-interactive properties of the tropoelastin-collagen composites; HT1080 cells, Rugli cells and human dermal fibroblasts (HDF). The relative tropoelastin and collagen-binding properties of these cell lines was investigated by coating tropoelastin onto tissue culture plastic (Figure 3). All three cell types showed high affinity for soluble collagen I and so this was used as a reference control. The three different cell types showed a differing affinity for tropoelastin with the trend HT1080 < HDF < Rugli cells. HT1080 cells possessed a low affinity for tropoelastin with a ~12 percentage point (pp) increase in cell adhesion when comparing 30 μg/mL tropoelastin coated tissue culture plastic against a non-coated control (Figure 3Ai). This was much lower than the ~76pp adhesion to a soluble collagen positive control. HDFs possessed intermediate affinity for tropoelastin with a ~50pp increase in cell adhesion on 30 μg/mL tropoelastin over non-coated controls (Figure 3Aii). Rugli cells showed the highest affinity for tropoelastin, where cell adhesion to 10 μg/mL tropoelastin was comparable to the soluble collagen positive control (Figure 3Aiii). Both HDFs and Rugli cells showed a flattened, spread morphology on 30 μg/mL tropoelastin coated tissue culture plastic (Figure 3 Bii and Biii respectively). By contrast HT1080 cells did not spread onto tropoelastin (Figure 3 Bi). All three cell lines possessed a flattened morphology on soluble collagen.

There are several tropoelastin receptors [13,15–19], so the tropoelastin receptor usage of each cell line was evaluated. As HT1080 cells showed low levels of cell adhesion on tropoelastin, the receptor class utilised by this cell line was not studied. Mg^{2+} supplementation and EDTA chelation of divalent cations are often used as a convenient method to activate or deactivate integrin mediated interactions respectively through the metal ion dependent adhesion site in integrins. HDF adhesion to both soluble collagen and tropoelastin coated tissue culture plastic was sensitive to inclusion of 5mM EDTA (Figure 3Ci), indicating an

integrin-mediated cell-adhesion mechanism. By contrast, Rugli cell adhesion to tropoelastin was not EDTA sensitive (Figure 3Cii). Further inhibition analysis using lactose (elastin binding protein inhibitor) and heparan sulfate (GAG-mediated interaction inhibitor) showed that Rugli cell adhesion to tropoelastin was sensitive to the inclusion of multiple inhibitors; suggesting that multiple tropoelastin-binding receptors are present on Rugli cells (Figure 3D). A combination of heparan sulfate and lactose inhibits Rugli cell adhesion by ~45pp over no-inhibitor controls. As each cell type utilises differing tropoelastin receptors, comparison between these three cell lines should allow us to determine which cell-adhesion mechanism(s) are being altered by tropoelastin addition to collagen biomaterials.

4.3. *Cell adhesion to tropoelastin-collagen composites.*

Initially the effect of including an increasing proportion of tropoelastin into collagen films was examined (Figure 4). As NHS/EDC crosslinking can modify cell adhesive sites in collagen [39], this analysis was conducted in the absence of NHS/EDC crosslinking or ethanol washing. The binding profile for all three cell lines was modified by the inclusion of tropoelastin into insoluble collagen films. For HT1080 cells and HDFs, the degree of cell adhesion in the presence of Mg^{2+} was unaffected by tropoelastin inclusion (solid line in Figure 4A and B respectively). By contrast, Rugli cell adhesion in the presence of Mg^{2+} increased from ~60% in the absence of tropoelastin to ~100% in with the inclusion of 0.5% (w/w) tropoelastin (solid line in Figure 4C). For all three cell lines, the inclusion of tropoelastin induced cell adhesion in the presence of 5mM EDTA (dashed lines in Figure 4). In the absence of tropoelastin, cell adhesion to the collagen film was completely inhibited by inclusion of 5mM EDTA, confirming that EDTA was inhibiting integrin-mediated cell adhesion to collagen. The degree of adhesion in the presence of EDTA increased dose-

dependently with increasing tropoelastin inclusion, saturating at 10% tropoelastin content for all three cell lines.

As cell adhesion in the presence of EDTA saturated with 20% (w/w) tropoelastin content, this was used to examine the combined effect of tropoelastin inclusion and NHS/EDC crosslinking (Figure 5). Both HT1080 cell and HDF cell adhesion showed a similar response to NHS/EDC crosslinking of tropoelastin-collagen composite films (Figure 5A and B respectively). NHS/EDC crosslinking partially inhibited cell adhesion to collagen-only films in the presence of Mg^{2+} by ~15-20pp of non-crosslinked values. This was not altered by the inclusion of 20% (w/w) tropoelastin. On collagen-only films, HT1080 cell and HDF adhesion in the presence of EDTA increased with NHS/EDC crosslinking. This was augmented by the presence of 20% (w/w) tropoelastin in the film, where EDTA-insensitive adhesion was higher on tropoelastin containing films. For HT1080 cells this was evident at all NHS/EDC concentrations, whereas for HDFs the degree of binding in the presence of EDTA saturated for both 20% tropoelastin-collagen composites and collagen-only films at 60% NHS/EDC crosslinking concentration. Rugli cell adhesion in the presence of Mg^{2+} was higher on the 20% (w/w) tropoelastin containing film than the collagen-only film (Figure 5C). This was evident for all NHS/EDC concentrations except 100% NHS/EDC and was particularly pronounced at 10% and 20% NHS/EDC. Similar to the other cell lines, Rugli cell adhesion in the presence of EDTA, to collagen-only films, increased with NHS/EDC crosslinking. This was elevated on the 20% (w/w) tropoelastin containing composites over the collagen-only films when crosslinked with between 0 and 20% NHS/EDC.

4.4. *Cell spreading and proliferation on tropoelastin-collagen composites.*

Engagement of cell receptors to the ECM can lead to cell signalling cascades and, in-turn, a cell morphological response. Therefore, cell area measurements were taken to

determine if tropoelastin inclusion was altering the cell morphology (Figure 6, Supplementary Figure 5). For Rugli cells, the cell area was approximately double on 20% (w/w) tropoelastin-containing films than on the collagen-only controls (Figure 6C). With NHS/EDC crosslinking the cell area decreased on both 20% (w/w) tropoelastin composites and collagen-only films, however the cell area was consistently larger on the 20% (w/w) tropoelastin containing composite for all NHS/EDC crosslinking concentrations. The Rugli cell aspect ratio was consistently larger on 20% tropoelastin-containing films compared to the collagen-only samples. This decreased with increasing EDC crosslinking (Supplementary Figure 5C). By contrast, the HT1080 and HDF cell area is predominantly affected by NHS/EDC crosslinking, with minimal impact from the inclusion of 20% (w/w) tropoelastin (Figure 6A,B respectively). HT1080 cell aspect ratio was unaffected by 20% tropoelastin inclusion (Supplementary Figure 5A), however HDF aspect ratio was lower on 20% tropoelastin-containing films when crosslinked with either 20% or 60% EDC (Supplementary Figure 5B). All three cell lines exhibited a large cell area on soluble collagen I or tissue culture plastic, confirming their spreading capacity. Therefore, tropoelastin inclusion can induce cell spreading and elongation in the Rugli cell line that adheres to tropoelastin via non-integrin-receptors.

The cell proliferative response on collagen-only and 20% (w/w) tropoelastin-collagen composites, crosslinked with increasing concentrations of NHS/EDC, was measured after 0, 3 and 5 days in culture (Figure 7). For all three cell lines, a similar number of cell nuclei were present at day 0, irrespective of tropoelastin inclusion or NHS/EDC crosslinking concentration. This proved uniform cell loading of the films. The HT1080 cell count at day 3 and 5 was dependent solely upon the degree of NHS/EDC crosslinking (Figure 7A). A slight increase in the cell count was observed on 10% and 20% NHS/EDC crosslinked films at day 5, however higher NHS/EDC concentrations inhibited cell proliferation. This was particularly

evident with 100% NHS/EDC crosslinking where the cell count was similar to day 0, suggesting limited cell proliferation. This trend was not altered by the inclusion of 20% (w/w) tropoelastin. The HT1080 cell morphology after 3 days in culture was indistinguishable between the 20% (w/w) tropoelastin composites and collagen-only controls (Supplementary Figure 6A). Instead, the morphology was strongly dependent upon NHS/EDC crosslinking.

HDF proliferation showed dependence upon NHS/EDC crosslinking and tropoelastin inclusion (Figure 7B). At day 3, in the absence of tropoelastin, the degree of cell proliferation increased with 10% and 20% NHS/EDC crosslinking and was inhibited with 60% and 100% NHS/EDC crosslinking. This trend was also somewhat evident at day 5; however, the formation of a complete monolayer at this time point resulted in smaller trends than at day 3. At day 3, the inclusion of 20% (w/w) tropoelastin did not alter HDF proliferation when combined with 0%, 10% and 100% NHS/EDC crosslinking. Conversely, 20% (w/w) tropoelastin inclusion increased HDF proliferation when combined with 20% NHS/EDC and, particularly, 60% NHS/EDC crosslinking. By day 5 the effect of 20% (w/w) tropoelastin inclusion was less evident at all NHS/EDC concentrations. At day 3 this effect was noticeable by fluorescence microscopy, where a more complete monolayer of cells was present on 20% (w/w) tropoelastin-containing films, compared to collagen-only controls when crosslinked with 60% NHS/EDC (Supplementary Figure 6B).

Rugli cell proliferation was strongly dependent upon tropoelastin inclusion (Figure 7C). At day 3, Rugli cell proliferation on collagen-only films was dependent upon NHS/EDC crosslinking, with minimal cell proliferation at 100% NHS/EDC crosslinking. The inclusion of 20% (w/w) tropoelastin did not alter cell proliferation over the collagen-only controls in the absence of NHS/EDC crosslinking. However, Rugli cell proliferation was markedly elevated, with approximately double the number of cell nuclei, on 20% (w/w) tropoelastin-

collagen composites, over collagen-only controls, when crosslinked with 10%, 20%, 60% and 100% NHS/EDC. Similarly, at day 5, Rugli cell proliferation was consistently elevated with 20% (w/w) tropoelastin inclusion at all NHS/EDC crosslinking concentrations. Fluorescent micrographs showed increased cell density on the 20% (w/w) tropoelastin containing films compared to the collagen-only films at day 3 (Supplementary Figure 6C). Additionally, 20% (w/w) tropoelastin inclusion minimised cell-cell clustering that dominates on collagen-only films crosslinked with 60% and 100% NHS/EDC. This was particularly evident after 5 days in culture (Supplementary Figure 6D).

5. Discussion

Producing materials that fully recapitulate the biofunctionality of the native ECM is a fundamental requirement of tissue engineering. In this study, collagen I and the elastic fibre precursor molecule, tropoelastin, were combined to mimic the ECM more closely. Each of these biologically-derived macromolecules possesses distinct cell-biological activity. Therefore, the response of 3 complementary cell lines (HT1080, Rugli and human dermal fibroblasts), each with differing elastin-binding receptor usage, was examined to delineate the relative contribution of collagen and elastin to the overall cellular response. This understanding of the cellular activity of tropoelastin and collagen, when combined as a composite, facilitates exploitation of the benefits of collagen (biophysical properties, biocompatibility, purity and cost) and tropoelastin (elastic recoil, cell phenotype guidance and non-thrombogenicity) within a single material, thus controlling the behaviour of specific cell types for tissue engineering and regenerative medicine.

5.1. *Composite fabrication.*

Several methods to incorporate tropoelastin into collagen-based materials were investigated. This included: 1) tropoelastin coating or drying onto precast collagen biomaterials, 2) tropoelastin addition during EDC crosslinking of collagen biomaterials and 3) co-blending tropoelastin into the collagen slurry prior to composite fabrication. All three methods incorporated tropoelastin into the collagen-based films (Figure 1, Supplementary Figure 1), however only composites fabricated by the co-blending approach retained tropoelastin after EDC crosslinking. EDC crosslinking is conducted in a 75% (v/v) ethanol solution, preventing collagen dispersion. Tropoelastin, by comparison, is comparatively solvent soluble, which is presumably why tropoelastin was eluted from the tropoelastin-coated collagen material (approach 1 above) during EDC crosslinking. By contrast,

tropoelastin that was co-blended into the collagen material is likely entwined and integrated into the collagen fibre matrix as seen previously for SE [6], hence is retained during crosslinking. As EDC crosslinking is vital for the long-term stability of collagen-based materials, the co-blending approach was used for the remainder of the study.

5.2. *Surface properties.*

When compared at the micron length scale, tropoelastin addition did not alter the surface topography of the collagen-based films (Figure 2, Supplementary Figure 2). This is similar to reports showing that SE does not significantly alter the surface roughness of collagen films, presumably as SE and tropoelastin form inter-collagen fibre amorphous materials [6,28] (Figure 1E). This differs from IE addition which, due to it being bulky and fibrous, significantly increases surface roughness [6,28]. At the micron length scale, tropoelastin addition results in the formation of ~50-200 nm rod-like structures, potentially due to tropoelastin self-association at high protein concentrations during film drying [44] (Supplementary Figure 3). The surface roughness was not systematically altered by EDC crosslinking [28] (Supplementary Figure 2B). QNM analysis of the surface showed that the median deformation of the films was increased by the addition of tropoelastin at 20%, which is consistent with reports showing that elastin addition decreases collagen-based bulk material stiffness [28,45] (Supplementary Figure 2A). In this study, the distribution of the more compliant tropoelastin-rich regions within the stiffer collagen matrix was assessed using QNM. The formation of spherical domains of high deformation observed in non-crosslinked films is consistent with the coacervation of tropoelastin into quantised protein spheres [41]. At high tropoelastin content in crosslinked samples, the films were comprised of localised yet highly compliant fibre networks. This is consistent with prior reports demonstrating crosslinking induced self-assembly into partially formed fibre bundles for both tropoelastin using lysyl oxidase [41] and collagen via EDC [46].

5.3. *Cell adhesion.*

As tropoelastin engages with different cell-surface receptors to collagen, cell behaviour on tropoelastin-collagen composites was examined. Three cell lines were chosen for this study. HDFs were used as their tropoelastin-binding capacity has been well established [19]. HT1080 and Rugli cells were included as they bind to collagen via single well characterised integrins. Unlike HDFs, the tropoelastin-binding capacity of HT1080 and Rugli cells is less well defined. For example, we have recently shown that HT1080 cells do not adhere to IE or SE [6], however tropoelastin-binding was unknown. Therefore, prior to studying the tropoelastin-collagen composites, we first analysed the tropoelastin-binding capacity of these 3 different cell lines, when tropoelastin was coated onto tissue culture plastic (Figure 3). This revealed that each cell line possessed distinctive tropoelastin-binding capacity where; HT1080 cells were tropoelastin insensitive, consistent with their low SE binding capacity [6]; fibroblasts adhered to tropoelastin via cell surface integrins, presumably previously identified α_V-containing integrins [16,18] and; Rugli cells adhered via non-integrin receptors such as cell-surface GAGs and the EBP which is different to SE [6]. This altered cell-binding profile suggests that differing cell-binding motifs in tropoelastin are being utilised by each cell line. For example, Rugli cell ligation to tropoelastin via HS and EBP, but not integrins, indicates use of HS-binding sites in exon 17-18 [17] or the C-terminus [15] of tropoelastin or VGVAPG motifs in exon 24 [14]. Conversely, integrin-mediated HDF-binding to tropoelastin may be via exons 12-16 [19] or the C-terminus [18]. As all sites are surface exposed, at different locations on tropoelastin [19], it is possible that each cell type is preferentially binding to a specific region of the tropoelastin molecule. The differing tropoelastin-binding properties of these cells allowed us to delineate the cell-surface receptor classes that were responsible for the cell-biological effects observed on tropoelastin-collagen composite materials. This analysis showed that cell adhesion in the absence of EDC

crosslinking was elevated only for the non-integrin receptor utilising, Rugli, cell line (Figure 4). This is comparable to SE containing films, albeit at much higher SE densities [6] and could be because HT1080 cells and HDFs bind maximally to non-crosslinked collagen, providing little scope for increased adhesion with the addition of tropoelastin. For all 3 cell lines, the degree of adhesion in the presence of the integrin-deactivating compound EDTA, increased with increasing tropoelastin content. The reason for this is unclear as HT1080 cells and fibroblasts did not bind to tropoelastin coated tissue culture plastic via non-integrin receptors. However, it is possible that when embedded into a collagen biomaterial, tropoelastin presents differently to cells than when it is bound to tissue culture plastic. Indeed, tropoelastin cell binding activity is extensively modulated by immobilisation to differing substrates [47]. As such, is it possible that when presented in a collagen network, tropoelastin can support non-integrin mediated cell binding that is not apparent when coated onto tissue culture plastic. Alternatively, tropoelastin addition could alter cell association through the collagen component as we have previously noted for IE and SE addition to collagen [6]. As the maximal effect was observed with 20% tropoelastin content, this was chosen to study EDC crosslinking of the tropoelastin-collagen composite. We observed that EDC ablated native-like cell binding to collagen-only films in the presence of Mg^{2+} (Figure 5). This is consistent with our previously described mechanism [39]. Instead, EDC induces adhesion that persisted in the presence of EDTA. The mechanism behind this effect is still under investigation. Tropoelastin addition elevated the degree of EDTA insensitive cell adhesion above EDC-crosslinking-induced levels (Figure 5). This was consistent with our finding that tropoelastin induces EDTA-insensitive adhesion to tropoelastin-collagen composites in the absence of EDC-crosslinking. As a result, tropoelastin increased adhesion of the Rugli cell line, that attaches to tropoelastin via non-integrin receptors, but not the other 2 cell types. It

also increased the proportion of EDTA-insensitive adhesion of all cell types, but not total cell adhesion.

5.4. *Cell morphology and proliferation.*

Receptor engagement by ECM molecules can result in the activation of cell signalling cascades, leading to morphological change. Although tropoelastin addition to collagen modifies the cell binding mechanism from EDTA sensitive to EDTA insensitive, the cell area was only altered for the Rugli cell line that adheres to tropoelastin via cell-surface GAGs and the EBP receptor (Figure 6). The increase in Rugli cell area is consistent with SE-containing films but is not evident on IE-containing films [6]. Interestingly HT1080 cell area is influenced by SE inclusion, but here we see no effect with tropoelastin addition. However, the HT1080 cell response to SE required 50% or greater SE content as 25% SE content had no effect. Here we use maximal 20% tropoelastin, and so the lack of HT1080 cell area response could be due to the lower elastin content used. This maximal tropoelastin content was chosen as films fabricated from a higher, 40% tropoelastin content were not stable under long-term cell culture conditions [data not shown]. The over 2-fold larger Rugli cell area in the presence of 20% tropoelastin indicates that these non-integrin tropoelastin receptors are inducing cell signalling. Rugli cells also possessed a larger aspect ratio on 20% tropoelastin-containing films (Supplementary Figure 5) indicating that tropoelastin is initiating cell signalling pathways. Elastin has been shown to activate numerous cell signalling pathways including activation of tyrosine kinases such as FAK, c-Src and platelet-derived growth factor receptor kinase which, in turn, signal via the Ras-Raf-MEK1/2-ERK1/2 phosphorylation cascade [48]. This was attributed to activation of the EBP which we have implicated in Rugli cell adhesion to tropoelastin. Therefore, it is possible that this same signalling pathway is activated by the addition of tropoelastin to collagen-based materials. EDC crosslinking inhibited cell spreading for all 3 cell lines on collagen-only or tropoelastin-

containing films. This is presumably due to EDC-modification of the cell-adhesion motifs in collagen [39]. These sites, such as the high affinity GFOGER motif, require coordination of the COOH group on the glutamic acid (E) side chain with a Mg^{2+} ion located in the I-domain contained within the α subunit of the integrin [49]. As glutamic acid side chains react with adjacent lysine side chains during EDC crosslinking, this results in modification of the critical glutamic acid side chains in the GxOGER motif in collagen, ablating integrin binding and cell signalling. For the Rugli cell line, tropoelastin increased the cell area and aspect ratio at all EDC-crosslinking densities (Figure 6, Supplementary Figure 5), indicating that, whilst cell signalling motifs in collagen are EDC-sensitive, those in tropoelastin are not. This is intriguing as the integrin-binding sequences in tropoelastin (TGTGVGPQA_7KA_3KFGAGAAGVLPGVGGAG, A_{10}KAAKYGA_3GL and RKRK [17–19]) contain EDC-susceptible lysine side groups, whilst VGVAPG sequences that ligate with the EBP receptor [14] do not. This could account for the bioactivity for cells utilising the non-integrin EBP receptor but not those utilising integrins after EDC crosslinking of the tropoelastin-collagen composites. Consistent with this explanation, tropoelastin inclusion into collagen-based materials induced proliferation of the non-integrin tropoelastin receptor utilising Rugli cell line, regardless of EDC crosslinking (Figure 7, Supplementary Figure 6). This is consistent with our prior findings that Rugli, but not HT1080, cell proliferation increased with SE but not IE incorporation when combined with 100% EDC crosslinking [6]. Fibroblasts showed an intermediary effect, where tropoelastin inclusion increased fibroblast proliferation, but only at 60% EDC crosslinking. It is intriguing to speculate why the incorporation of the integrin α_V binding sequences in tropoelastin has such a minimal effect on HT1080 cells and HDFs. For HT1080 cells this may simply reflect the low affinity of this cell line for tropoelastin (Figure 3Ai). However, fibroblasts adhere to tropoelastin via cell-surface integrins (Figure 3) but minimal impact was observed when tropoelastin was

incorporated into collagen films. This may reflect the fact that HDFs are ligating with both the collagen and incorporated tropoelastin components via the same class of receptors, integrins. As such, integrin-initiated signalling cascades may be activated by collagen alone, with no further capacity for activation by tropoelastin incorporation. Conversely Rugli cells were sensitive to tropoelastin incorporation, where these cells are ligating with tropoelastin via non-integrin receptors. As these non-integrin tropoelastin receptors do not bind to collagen they could activate alternate signalling cascades compared to collagen alone, initiating cellular effects when tropoelastin is present.

In summary, comparison of these three cell lines has delineated the relative contribution of tropoelastin and collagen ligation in the cellular response to a composite tropoelastin-collagen material. We found that, when present, non-integrin cell surface tropoelastin receptors dominate the cellular response to the tropoelastin component. This new understanding allows for bespoke materials design, tailored for specific cell types, that ligate with known receptor classes with advantages for tissue engineering and regenerative medicine.

6. Conclusions

Tropoelastin was incorporated into collagen-based materials using a co-blending approach, ensuring persistence during subsequent EDC-crosslinking reactions. Use of three different cell lines, with low (HT1080), intermediate (HDFs), and high affinity (Rugli) for tropoelastin, allowed us to define the relative impact of tropoelastin inclusion on collagen biomaterial bioactivity and to assign the impact of EDC-crosslinking. The inclusion of tropoelastin heavily influences the proliferation and morphology of Rugli cells utilising non-integrin cell-surface tropoelastin receptors. Although tropoelastin inclusion altered cell binding from EDTA–sensitive to EDTA-insensitive, this did not result in morphological changes in HDFs, that bind to tropoelastin via cell-surface integrins, or the morphology and proliferation of HT1080 cells that are devoid of tropoelastin receptors. We have discovered that cell-surface non-integrin tropoelastin-receptors heavily influence the cellular response to tropoelastin-collagen composite biomaterials, whereas tropoelastin-binding integrins have marginal impact. This knowledge permits composite tropoelastin-collagen design to control the cellular response.

7. Acknowledgements

This work was supported by the EPSRC fellowship EP/N019938/1 and ERC Advanced Grant 320598 3D-E and the 3DBioNet. D. V. Bax was funded by the Peoples Programme of the EU 7th Framework Programme (RAE no: PIIF-GA-2013-624904). M.N. acknowledges Emmanuel College (University of Cambridge) for funding. MN would like to thank Dr Sohini Kar-Narayan for access to the Multi Mode 8 scanning probe microscope.

8. References

[1] C.H. Lee, A. Singla, Y. Lee, Biomedical applications of collagen., Int. J. Pharm. 221 (2001) 1–22.

[2] C. Frantz, K.M. Stewart, V.M. Weaver, The extracellular matrix at a glance, J. Cell Sci. 123 (2010) 4195–4200.

[3] P. Bornstein, Matricellular proteins: An overview, J. Cell Commun. Signal. 3 (2009) 163–165.

[4] N. Afratis, C. Gialeli, D. Nikitovic, T. Tsegenidis, E. Karousou, A.D. Theocharis, M.S. Pavão, G.N. Tzanakakis, N.K. Karamanos, Glycosaminoglycans: Key players in cancer cell biology and treatment, FEBS J. 279 (2012) 1177–1197.

[5] L.C. Abraham, E. Zuena, B. Perez-Ramirez, D.L. Kaplan, Guide to collagen characterization for biomaterial studies., J. Biomed. Mater. Res. B. Appl. Biomater. 87 (2008) 264–285.

[6] D. V. Bax, H.E. Smalley, R.W. Farndale, S.M. Best, R.E. Cameron, Cellular response to collagen-elastin composite materials, Acta Biomater. 86 (2019) 158–170.

[7] J. Xu, G.P. Shi, Vascular wall extracellular matrix proteins and vascular diseases, Biochim. Biophys. Acta - Mol. Basis Dis. 1842 (2014) 2106–2119.

[8] K.E. Kadler, C. Baldock, J. Bella, R.P. Boot-Handford, Collagens at a glance, J. Cell Sci. 120 (2007) 1955–1958.

[9] J. Uitto, Biochemistry of the elastic fibers in normal connective tissues and its alterations in diseases, J. Invest. Dermatol. 72 (1979) 1–10.

[10] C.B. Saitow, S.G. Wise, A.S. Weiss, J.J. Castellot, D.L. Kaplan, Elastin biology and tissue engineering with adult cells, Biomol. Concepts. 4 (2013) 173–185.

[11] G.C. Yeo, A.S. Weiss, Soluble matrix protein is a potent modulator of mesenchymal

stem cell performance, Proc. Natl. Acad. Sci. U. S. A. 116 (2019) 2042–2051.

[12] J. Holst, S. Watson, M.S. Lord, S.S. Eamegdool, D.V. Bax, L.B. Nivison-Smith, A. Kondyurin, L. Ma, A.F. Oberhauser, A.S. Weiss, J.E.J. Rasko, Substrate elasticity provides mechanical signals for the expansion of hemopoietic stem and progenitor cells, Nat. Biotechnol. 28 (2010) 1123-1128.

[13] R.P. Mecham, A. Hinek, R. Entwistle, D.S. Wrenn, G.L. Griffin, R.M. Senior, Elastin binds to a multifunctional 67-kilodalton peripheral membrane protein, Biochemistry. 28 (1989) 3716–3722.

[14] R.M. Senior, G.L. Griffin, R.P. Mecham, D.S. Wrenn, K.U. Prasad, D.W. Urry, Val-Gly-Val-Ala-Pro-Gly, a repeating peptide in elastin, is chemotactic for fibroblasts and monocytes., J. Cell Biol. 99 (1984) 870–874.

[15] T.J. Broekelmann, B.A. Kozel, H. Ishibashi, C.C. Werneck, F.W. Keeley, L. Zhang, R.P. Mecham, Tropoelastin interacts with cell-surface glycosaminoglycans via its COOH-terminal domain., J. Biol. Chem. 280 (2005) 40939–40947.

[16] P. Lee, D. V. Bax, M.M.M. Bilek, A.S. Weiss, A novel cell adhesion region in tropoelastin mediates attachment to integrin αVβ5, J. Biol. Chem. 289 (2014) 1467–1477.

[17] P. Lee, G.C. Yeo, A.S. Weiss, A cell adhesive peptide from tropoelastin promotes sequential cell attachment and spreading via distinct receptors, FEBS J. 284 (2017) 2216–2230.

[18] D.V. Bax, U.R. Rodgers, M.M.M. Bilek, A.S. Weiss, Cell adhesion to tropoelastin is mediated via the C-terminal GRKRK motif and integrin αvβ3, J. Biol. Chem. 284 (2009) 28616-28623.

[19] B. Bochicchio, G.C. Yeo, P. Lee, D. Emul, A. Pepe, A. Laezza, N. Ciarfaglia, D. Quaglino, A.S. Weiss, Domains 12 to 16 of tropoelastin promote cell attachment and

spreading through interactions with glycosaminoglycan and integrins alphaV and alpha5beta1, FEBS J. (2021) febs.15702.

[20] J.D. Humphries, A. Byron, M.J. Humphries, Integrin ligands at a glance, J. Cell Sci. 119 (2006) 3901–3903.

[21] S. Hamaia, R.W. Farndale, Integrin recognition motifs in the human collagens, Adv. Exp. Med. Biol. 819 (2014) 127–142.

[22] J.F. Almine, D. V. Bax, S.M. Mithieux, L. Nivison-Smith, J. Rnjak, A. Waterhouse, S.G. Wise, A.S. Weiss, Elastin-based materials, Chem. Soc. Rev. 39 (2010) 3371–3379.

[23] T. Broekelmann, C. Ciliberto, A. Shifren, R. Mecham, Modification and functional inactivation of the tropoelastin carboxy-terminal domain in cross-linked elastin, Matrix Biol. 27 (2008) 631–639.

[24] D.T. Simionescu, Q. Lu, Y. Song, J.S. Lee, T.N. Rosenbalm, C. Kelley, N.R. Vyavahare, Biocompatibility and remodeling potential of pure arterial elastin and collagen scaffolds., Biomaterials. 27 (2006) 702–713.

[25] J. Rnjak-Kovacina, S.G. Wise, Z. Li, P.K.M. Maitz, C.J. Young, Y. Wang, A.S. Weiss, Tailoring the porosity and pore size of electrospun synthetic human elastin scaffolds for dermal tissue engineering, Biomaterials. 32 (2011) 6729–6736.

[26] A.J. Ryan, F.J. O'Brien, Insoluble elastin reduces collagen scaffold stiffness, improves viscoelastic properties, and induces a contractile phenotype in smooth muscle cells., Biomaterials. 73 (2015) 296–307.

[27] J. Skopinska-Wisniewska, A. Sionkowska, A. Kaminska, A. Kaznica, R. Jachimiak, T. Drewa, Surface characterization of collagen/elastin based biomaterials for tissue regeneration, Appl. Surf. Sci. 255 (2009) 8286–8292.

[28] C.N. Grover, R.W. Farndale, S.M. Best, R.E. Cameron, The interplay between

physical and chemical properties of protein films affects their bioactivity, J. Biomed. Mater. Res. Part A. 100 (2012) 2401–2411.

[29] C.N. Grover, R.E. Cameron, S.M. Best, Investigating the morphological, mechanical and degradation properties of scaffolds comprising collagen, gelatin and elastin for use in soft tissue engineering, J. Mech. Behav. Biomed. Mater. 10 (2012) 62–74.

[30] W.F. Daamen, H.T.B. van Moerkerk, T. Hafmans, L. Buttafoco, A.A. Poot, J.H. Veerkamp, T.H. van Kuppevelt, Preparation and evaluation of molecularly-defined collagen-elastin-glycosaminoglycan scaffolds for tissue engineering., Biomaterials. 24 (2003) 4001–4009.

[31] W.F. Daamen, S.T.M. Nillesen, T. Hafmans, J.H. Veerkamp, M.J.A. van Luyn, T.H. van Kuppevelt, Tissue response of defined collagen-elastin scaffolds in young and adult rats with special attention to calcification., Biomaterials. 26 (2005) 81–92.

[32] A.T. Nguyen, S.R. Sathe, E.K.F. Yim, From nano to micro: topographical scale and its impact on cell adhesion, morphology and contact guidance, J. Phys. Condens. Matter. 28 (2016) 183001.

[33] A. Waterhouse, S.G. Wise, M.K.C. Ng, A.S. Weiss, Elastin as a nonthrombogenic biomaterial., Tissue Eng. Part B. Rev. 17 (2011) 93–99.

[34] M. Meyer, Processing of collagen based biomaterials and the resulting materials properties, Biomed. Eng. Online. 18 (2019) 24.

[35] K. Adamiak, A. Sionkowska, Current methods of collagen cross-linking: Review, Int. J. Biol. Macromol. 161 (2020) 550–560.

[36] N. Davidenko, C.F. Schuster, D.V. Bax, N. Raynal, R.W. Farndale, S.M. Best, R.E. Cameron, Control of crosslinking for tailoring collagen-based scaffolds stability and mechanics, Acta Biomater. 25 (2015) 131–142.

[37] L.H. Olde Damink, P.J. Dijkstra, M.J. van Luyn, P.B. van Wachem, P. Nieuwenhuis, J.

Feijen, Cross-linking of dermal sheep collagen using a water-soluble carbodiimide., Biomaterials. 17 (1996) 765–773.

[38] R.W. Farndale, T. Lisman, D. Bihan, S. Hamaia, C.S. Smerling, N. Pugh, A. Konitsiotis, B. Leitinger, P.G. de Groot, G.E. Jarvis, N. Raynal, Cell–collagen interactions: the use of peptide Toolkits to investigate collagen–receptor interactions, Biochem. Soc. Trans. 36 (2008) 241–250.

[39] D. V. Bax, N. Davidenko, D. Gullberg, S.W. Hamaia, R.W. Farndale, S.M. Best, R.E. Cameron, Fundamental insight into the effect of carbodiimide crosslinking on cellular recognition of collagen-based scaffolds, Acta Biomater. 49 (2017) 218–234.

[40] C. Baldock, A.F. Oberhauser, L. Ma, D. Lammie, V. Siegler, S.M. Mithieux, Y. Tu, J.Y.H. Chow, F. Suleman, M. Malfois, S. Rogers, L. Guo, T.C. Irving, T.J. Wess, A.S. Weiss, Shape of tropoelastin, the highly extensible protein that controls human tissue elasticity, Proc. Natl. Acad. Sci. U. S. A. 108 (2011) 4322–4327.

[41] S.M. Mithieux, Y. Tu, E. Korkmaz, F. Braet, A.S. Weiss, In situ polymerization of tropoelastin in the absence of chemical cross-linking, Biomaterials. 30 (2009) 431–435.

[42] U.R. Rodgers, A.S. Weiss, Integrin αvβ3 binds a unique non-RGD site near the C-terminus of human tropoelastin, Biochimie. 86 (2004) 173–178.

[43] A.W. Clarke, E.C. Arnspang, S.M. Mithieux, E. Korkmaz, F. Braet, A.S. Weiss, Tropoelastin massively associates during coacervation to form quantized protein spheres, Biochemistry. 45 (2006) 9989–9996.

[44] L.D. Muiznieks, S. Sharpe, R. Pomès, F.W. Keeley, Role of Liquid–Liquid Phase Separation in Assembly of Elastin and Other Extracellular Matrix Proteins, J. Mol. Biol. 430 (2018) 4741–4753.

[45] T.-U. Nguyen, C.A. Bashur, V. Kishore, Impact of elastin incorporation into

electrochemically aligned collagen fibers on mechanical properties and smooth muscle cell phenotype., Biomed. Mater. 11 (2016) 025008.

[46] M. Nair, Y. Calahorra, S. Kar-Narayan, S.M. Best, R.E. Cameron, Self-assembly of collagen bundles and enhanced piezoelectricity induced by chemical crosslinking, Nanoscale. 11 (2019) 15120–15130.

[47] D.V. Bax, D.R. McKenzie, M.M.M. Bilek, A.S. Weiss, Directed cell attachment by tropoelastin on masked plasma immersion ion implantation treated PTFE, Biomaterials. 32 (2011) 6710-6718.

[48] S. Mochizuki, B. Brassart, A. Hinek, Signaling pathways transduced through the elastin receptor facilitate proliferation of arterial smooth muscle cells, J. Biol. Chem. 277 (2002) 44854–44863.

[49] J. Emsley, C.G. Knight, R.W. Farndale, M.J. Barnes, R.C. Liddington, Structural basis of collagen recognition by integrin α2β1, Cell. 101 (2000) 47–56.

9. Legends

Table 1 : Strategies to incorporate tropoelastin into collagen-biomaterials.

Figure 1 : BA-4 anti-elastin antibody detection of tropoelastin (TE) incorporated into collagen films. ELISA detection (**A-C**) of tropoelastin deposition from a solution onto collagen films prior to crosslinking (**A**) or of 50 µg/mL tropoelastin coated collagen films treated with increasing concentrations of NHS/EDC (**B**). Positive control tropoelastin detection in the absence of crosslinking solution is shown. (**C**) when blended at increasing concentration (shown as % of total protein content) into the collagen slurry prior to film casting. Films were either non-crosslinked (non-XL) or crosslinked with 100% EDC (100% EDC). (**D-E**) Immunofluorescent quantification (**D**) and representative images (**E**) of tropoelastin when blended into the collagen slurry prior to casting and crosslinked with 100% EDC. Negative no primary antibody and Bovine Serum Albumin (BSA) controls and positive tropoelastin-coated tissue culture plastic (TCP) are shown. Scale bar = 200 µm. Error bars indicate S.D. of triplicate (**A-C**) or quintuplicate (**D**) measurements.

Figure 2 : Atomic force microscopy of the surface topography (left of each pair of images) and deformation (right of each pair of images) of tropoelastin-collagen composite films containing an increasing proportion of tropoelastin (expressed as % of total protein content). The films were either non-crosslinked or 100% EDC crosslinked. The scale bar indicates 1 µm.

Figure 3 : (**A,B**) HT1080 (**i**), Human Dermal Fibroblast (HDF –**ii**), and Rugli (**iii**) cell response to tropoelastin (TE) coated onto tissue culture plastic surfaces. (**A**) Cell attachment to tropoelastin coated onto tissue culture plastic at increasing concentrations. Negative

control adhesion to bovine serum albumin (BSA) and positive control adhesion to 5 μg/mL soluble collagen coated tissue culture plastic (CN) are shown. (**B**) Phase contrast micrographs of cell spreading onto tissue culture plastic coated with 0, 5 and 30 μg/mL tropoelastin or 5 μg/mL soluble collagen I. (**C**) Inhibition of HDF (**i**) or Rugli (**ii**) cell adhesion to 30 μg/mL tropoelastin or 5 μg/mL collagen coated tissue culture plastic in the presence or absence of 5 mM EDTA. (**D**) Inhibition of Rugli cell adhesion to 30 μg/mL tropoelastin or 5 μg/mL soluble collagen I coated tissue culture plastic by the presence of combinations of 5 mM EDTA (inhibits integrins), 5 mM β-lactose (lac; inhibits elastin binding protein) or 10 μg/mL heparan sulfate (HS; inhibits GAG-mediated binding). For all figures, non-specific adhesion to the culture plate was blocked with BSA. Scale bar = 200 μm. Error bars indicate S.D. of quadruplicate (**A,B, Ci**) or triplicate (**Cii,D**) measurements.

Figure 4 : HT1080 (**A**), human dermal fibroblast (HDF – **B**), or Rugli (**C**), cell attachment to collagen films containing an increasing proportion of tropoelastin (expressed as a percentage of the total protein mass). Cell adhesion was measured in the presence of 5 mM Mg^{2+} or 5 mM EDTA. Non-specific adhesion to the culture plate was blocked with bovine serum albumin. Films were not EDC-crosslinked. Error bars indicate S.D. of triplicate measurements. Notations show significance from the 0% tropoelastin values for each data point, respectively. To aid legibility, control adhesion to soluble collagen (CN) or bovine serum albumin are shown separately.

Figure 5 : HT1080 (**A**), human dermal fibroblast (HDF – **B**), or Rugli (**C**) cell attachment to collagen-only films (No TE) and collagen films containing 20% (w/w) tropoelastin (20% TE) crosslinked with increasing concentrations of EDC in the presence of 5 mM Mg^{2+} or 5 mM EDTA. Non-specific adhesion to the culture plate was blocked with bovine serum albumin.

Error bars indicate S.D. of triplicate measurements. To aid legibility, control adhesion to soluble collagen (CN) or tissue culture plastic (TCP) are shown separately.

Figure 6 : HT1080 (**A**), human dermal fibroblast (HDF – **B**), or Rugli (**C**) cell area on collagen-only films (No TE) or collagen films containing 20% (w/w) tropoelastin (20% TE) crosslinked with increasing concentrations of EDC. Controls on tissue culture plastic or 5 µg/mL soluble collagen I are shown separately. Non-specific cell spreading was blocked with bovine serum albumin. Error bars indicate S.D. of six replicates. Notation show significance between No TE and 20% TE values for each EDC concentration respectively.

Figure 7 : Cell nuclei count/field of view of HT1080 (**A**), human dermal fibroblast (HDF – **B**), or Rugli (**C**) cells after 0 (**i**), 3 (**ii**), and 5 (**iii**) days in culture on collagen-only films (No TE) and collagen films containing 20% (w/w) tropoelastin (20% TE) crosslinked with increasing concentrations of EDC. Tissue culture plastic (TCP) and 5 µg/mL soluble collagen I (Sol CN) controls are shown. Error bars indicate S.D. of six replicates. Notations show significance between no-TE and 20% TE values for each EDC concentration respectively. The legend for all graphs is shown at the top of the figure.

Table 1

	1. Co-blend tropoelastin:collagen films	**2. Tropoelastin coating collagen films prior to crosslinking**	**3. Tropoelastin coating during crosslinking**
Cast material 200 µL/48-well plates (Starlab) or 100 µL/ 13 mm diameter glass coverslips or 1 cm^2 glass slides	Manual mixing a 1:1 ratio of 1 wt% collagen slurry (final collagen density = 0.5 wt%) and appropriate concentration of tropoelastin in 0.05 M acetic acid (tropoelastin defined as a % of the collagen content).	Manual mixing a 1:1 ratio of 1 wt% collagen slurry and 0.05 M acetic acid (final collagen density = 0.5 wt%).	Manual mixing a 1:1 ratio of 1 wt% collagen slurry and 0.05 M acetic acid (final collagen density = 0.5 wt%).
Film drying	48 hours in fume hood at room temperature		
Tropoelastin coating	None	400 µL of 50 µg/mL tropoelastin in 75% (v/v) ethanol. The ethanol was evaporated in a laminar flow hood,	None
EDC/NHS crosslinking 100% = molar ratio of 5 EDC : 2 NHS in 75% (v/v) ethanol. (30mM EDC).	Crosslinker diluted to appropriate concentration from the 100% solution with 75% (v/v) ethanol. Films were crosslinked at room temperature for 2 h	Crosslinker diluted to appropriate concentration from the 100% solution with 75% (v/v) ethanol. Films were crosslinked at room temperature for 2 h	50 µg/mL tropoelastin added to 100% crosslinking volume. Films were crosslinked at room temperature for 2 h
Washing	Extensively with deionised water		
Final drying	48 hours in fume hood at room temperature		

Figure 1

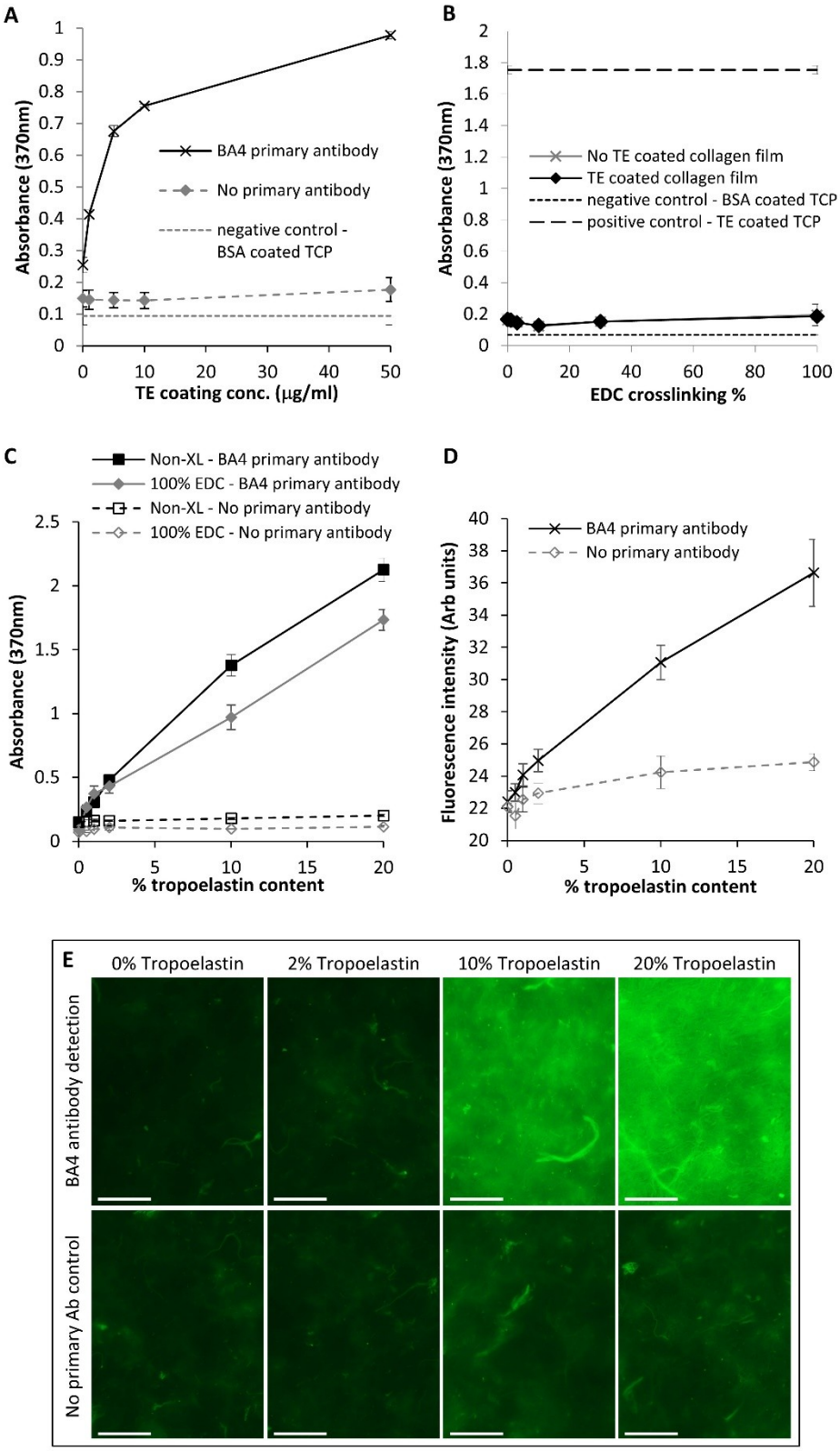
A
Absorbance (370nm)
TE coating conc. (µg/ml)
BA4 primary antibody
No primary antibody
negative control - BSA coated TCP
B
Absorbance (370nm)
EDC crosslinking %
No TE coated collagen film
TE coated collagen film
negative control - BSA coated TCP
positive control - TE coated TCP
C
Absorbance (370nm)
% tropoelastin content
Non-XL - BA4 primary antibody
100% EDC - BA4 primary antibody
Non-XL - No primary antibody
100% EDC - No primary antibody
D
Fluorescence intensity (Arb units)
% tropoelastin content
BA4 primary antibody
No primary antibody
E
0% Tropoelastin
2% Tropoelastin
10% Tropoelastin
20% Tropoelastin
BA4 antibody detection
No primary Ab control

Figure 2

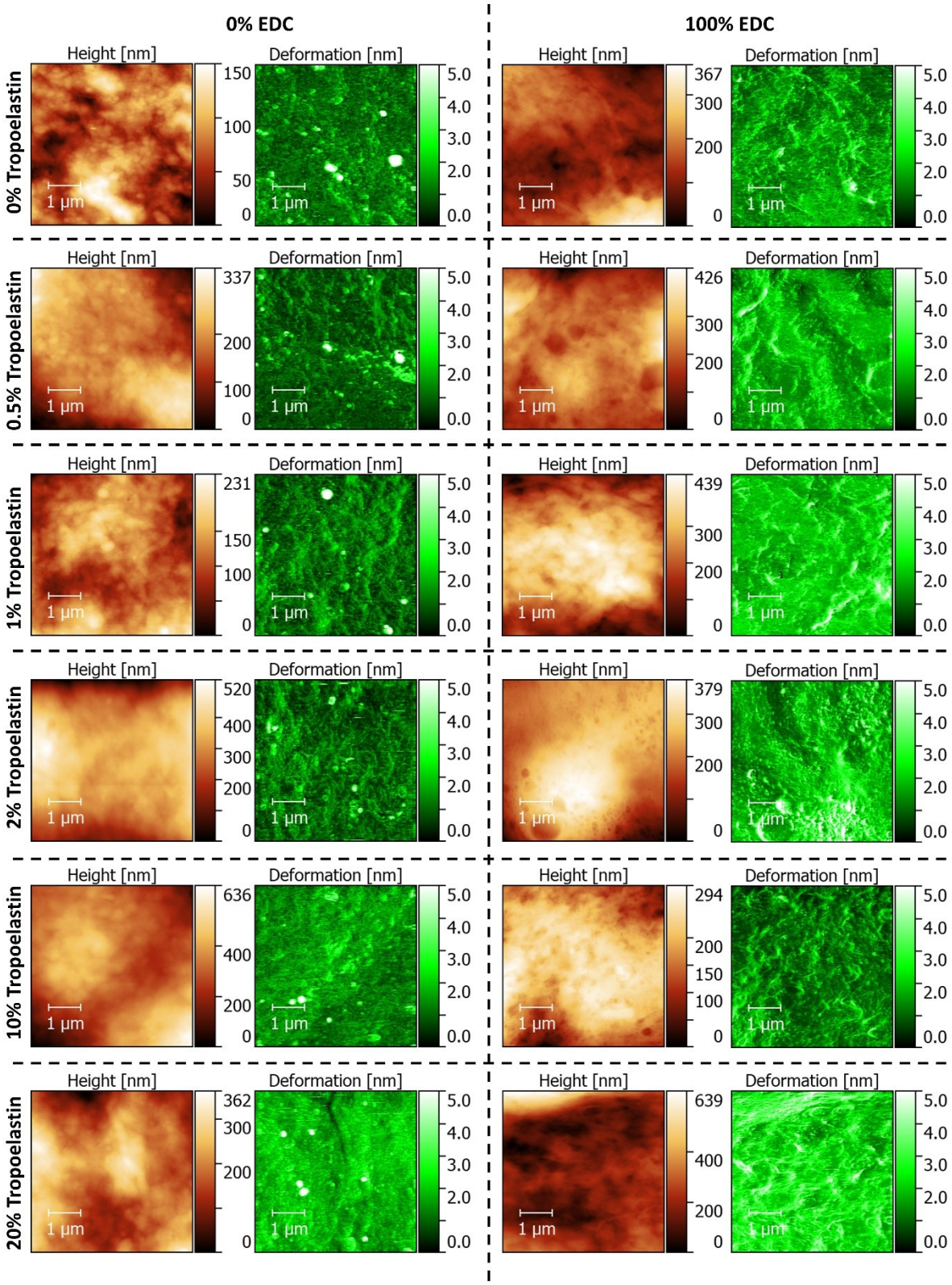
0% EDC
100% EDC
0% Tropoelastin
0.5% Tropoelastin
1% Tropoelastin
2% Tropoelastin
10% Tropoelastin
20% Tropoelastin
Height [nm]
Deformation [nm]
1 µm
150
100
50
0
337
200
231
520
400
300
636
362
367
426
439
379
294
639
5.0
4.0
3.0
2.0
0.0

Figure 3

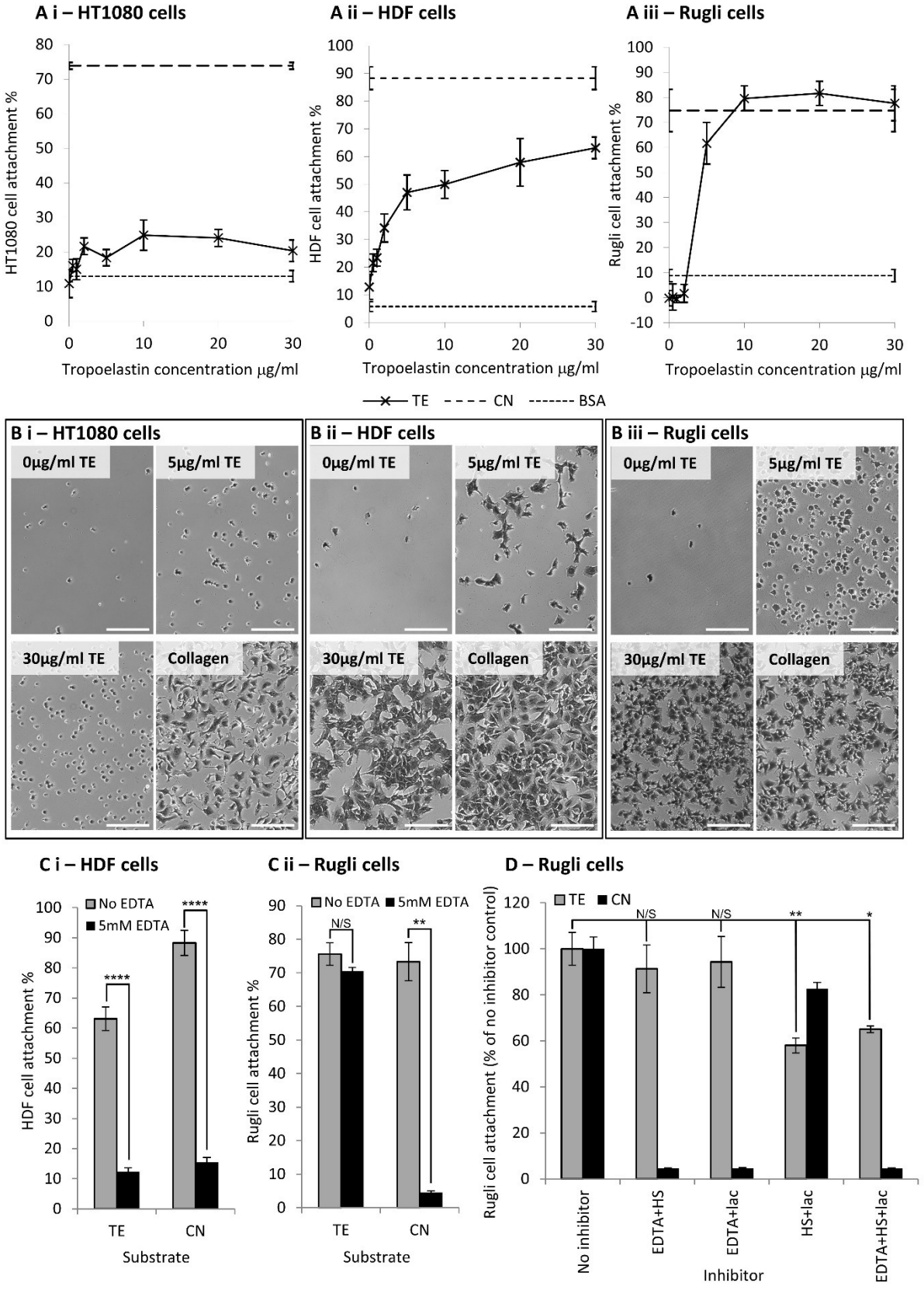
A i – HT1080 cells
A ii – HDF cells
A iii – Rugli cells
HT1080 cell attachment %
HDF cell attachment %
Rugli cell attachment %
Tropoelastin concentration µg/ml
TE
CN
BSA
B i – HT1080 cells
B ii – HDF cells
B iii – Rugli cells
0µg/ml TE
5µg/ml TE
30µg/ml TE
Collagen
C i – HDF cells
C ii – Rugli cells
No EDTA
5mM EDTA
N/S
Substrate
D – Rugli cells
Rugli cell attachment (% of no inhibitor control)
No inhibitor
EDTA+HS
EDTA+lac
HS+lac
EDTA+HS+lac
Inhibitor

Figure 4

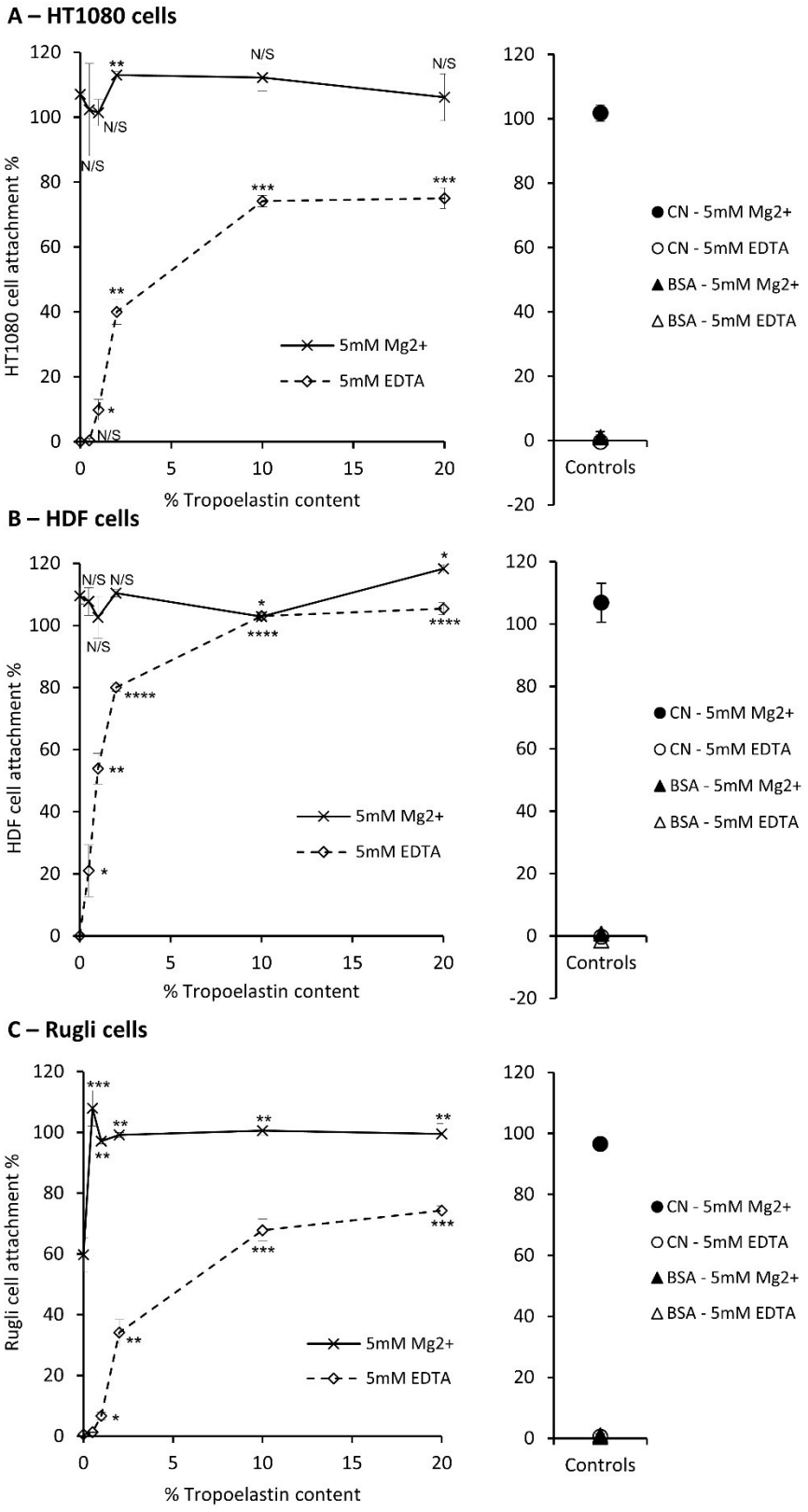
A – HT1080 cells
HT1080 cell attachment %
% Tropoelastin content
5mM Mg2+
5mM EDTA
Controls
CN - 5mM Mg2+
CN - 5mM EDTA
BSA - 5mM Mg2+
BSA - 5mM EDTA
B – HDF cells
HDF cell attachment %
% Tropoelastin content
5mM Mg2+
5mM EDTA
Controls
CN - 5mM Mg2+
CN - 5mM EDTA
BSA - 5mM Mg2+
BSA - 5mM EDTA
C – Rugli cells
Rugli cell attachment %
% Tropoelastin content
5mM Mg2+
5mM EDTA
Controls
CN - 5mM Mg2+
CN - 5mM EDTA
BSA - 5mM Mg2+
BSA - 5mM EDTA

Figure 5

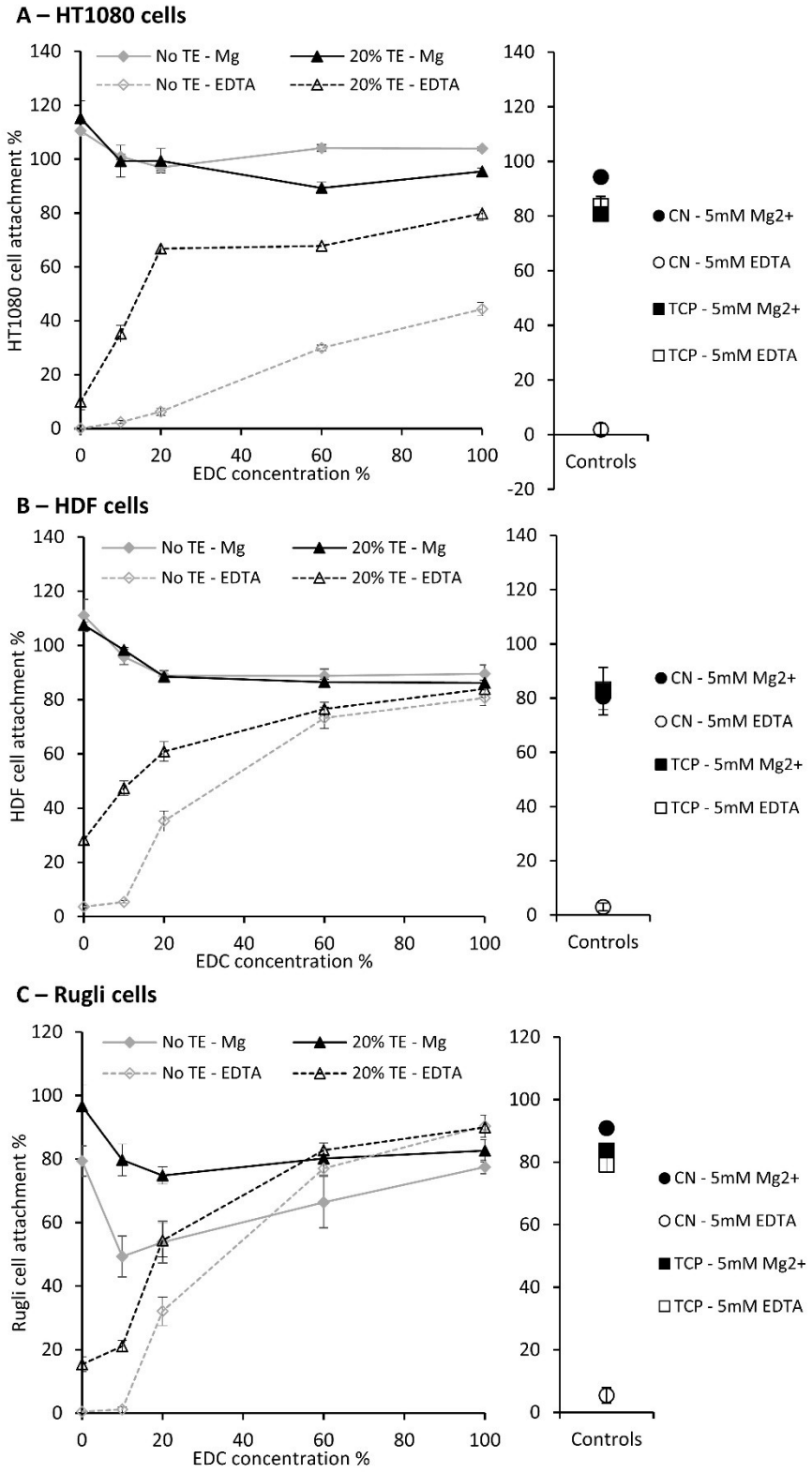
A – HT1080 cells
No TE - Mg
20% TE - Mg
No TE - EDTA
20% TE - EDTA
HT1080 cell attachment %
EDC concentration %
Controls
CN - 5mM Mg2+
CN - 5mM EDTA
TCP - 5mM Mg2+
TCP - 5mM EDTA
B – HDF cells
HDF cell attachment %
C – Rugli cells
Rugli cell attachment %

Figure 6

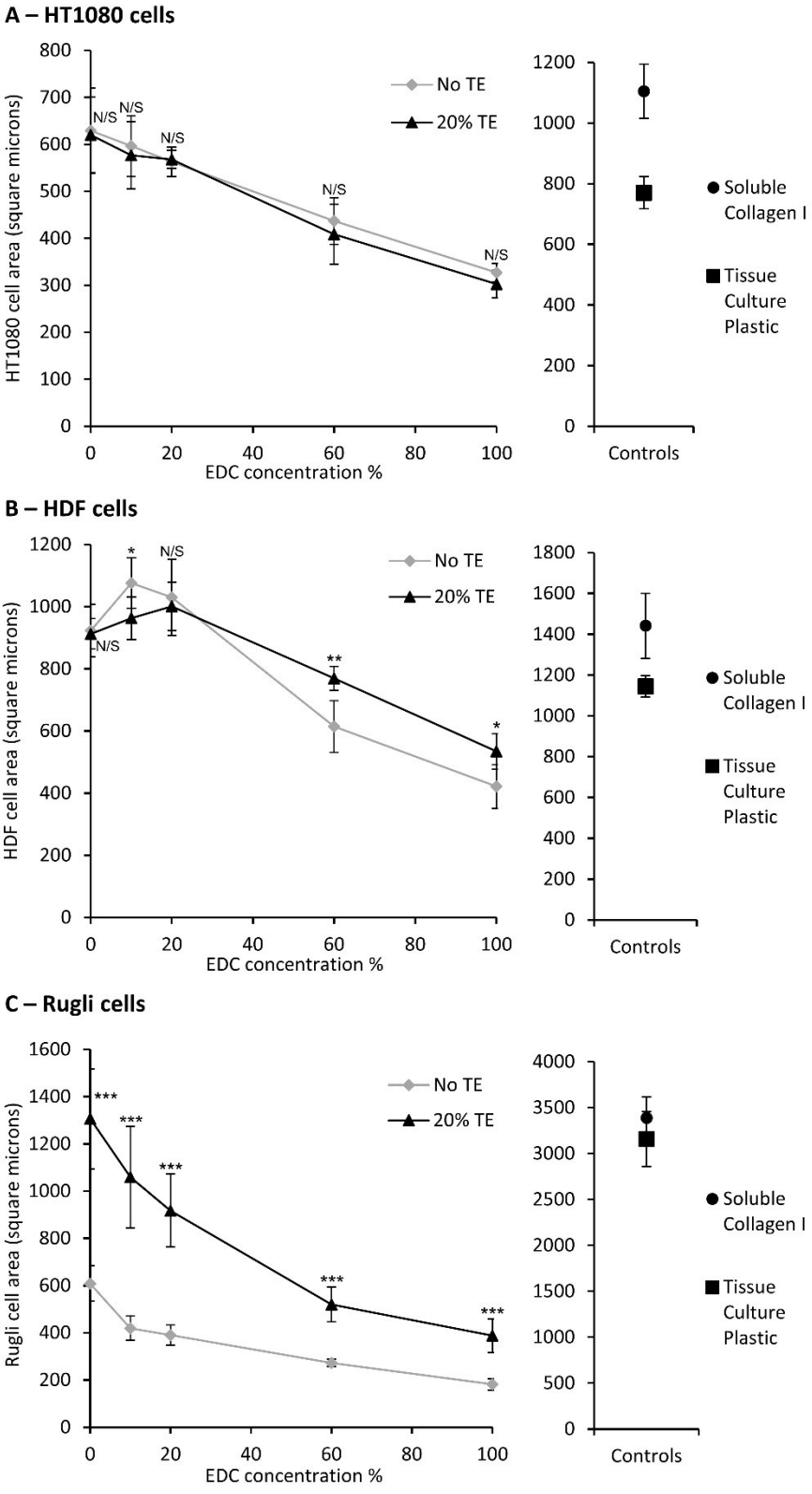
A – HT1080 cells
HT1080 cell area (square microns)
EDC concentration %
No TE
20% TE
N/S
Controls
Soluble Collagen I
Tissue Culture Plastic
B – HDF cells
HDF cell area (square microns)
EDC concentration %
No TE
20% TE
N/S
*
**
Controls
Soluble Collagen I
Tissue Culture Plastic
C – Rugli cells
Rugli cell area (square microns)
EDC concentration %
No TE
20% TE
***
Controls
Soluble Collagen I
Tissue Culture Plastic

Figure 7

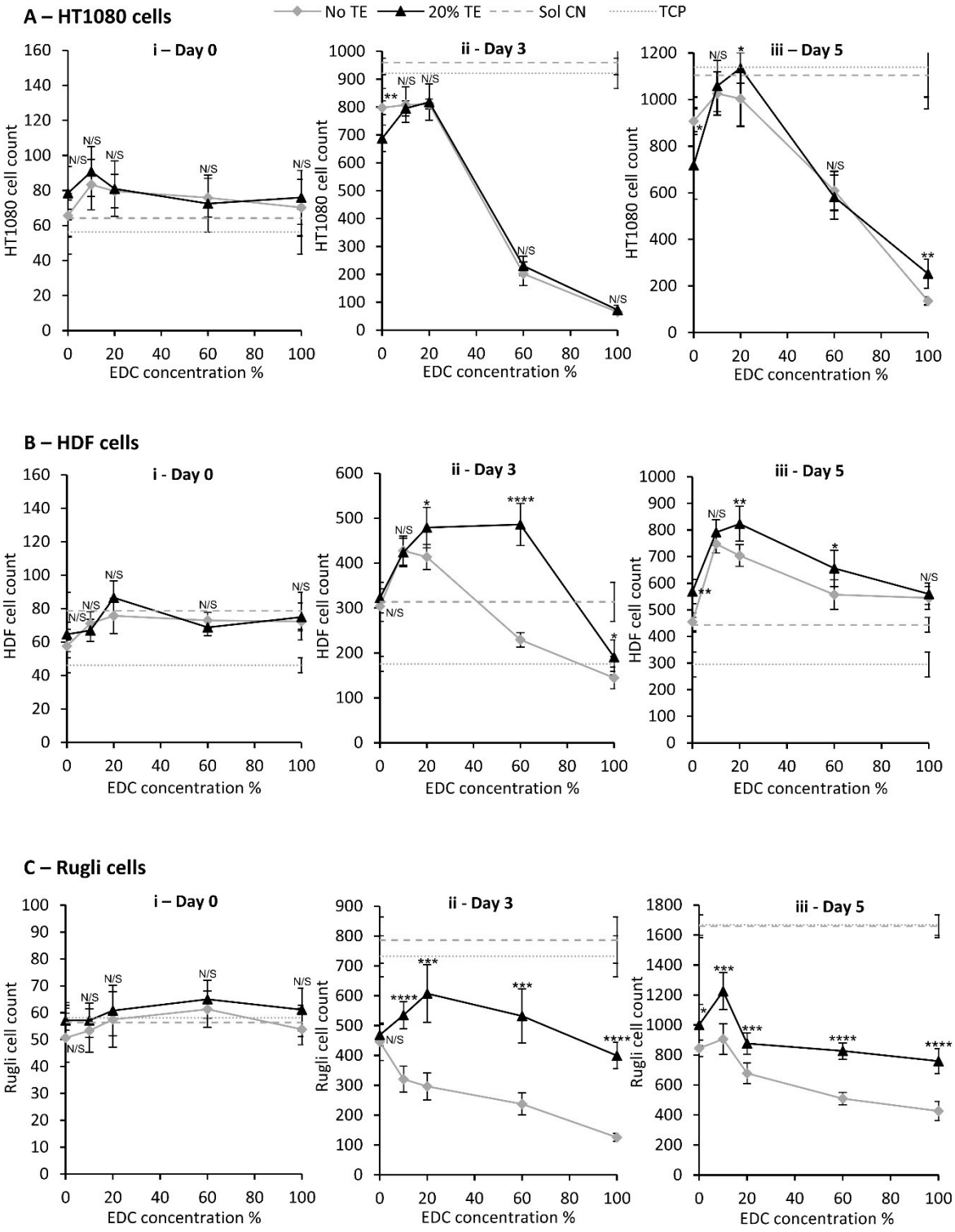
A – HT1080 cells
No TE
20% TE
Sol CN
TCP
i – Day 0
ii - Day 3
iii – Day 5
HT1080 cell count
EDC concentration %
B – HDF cells
i - Day 0
ii - Day 3
iii - Day 5
HDF cell count
EDC concentration %
C – Rugli cells
i – Day 0
ii - Day 3
iii - Day 5
Rugli cell count
EDC concentration %

Supplementary Figure 1

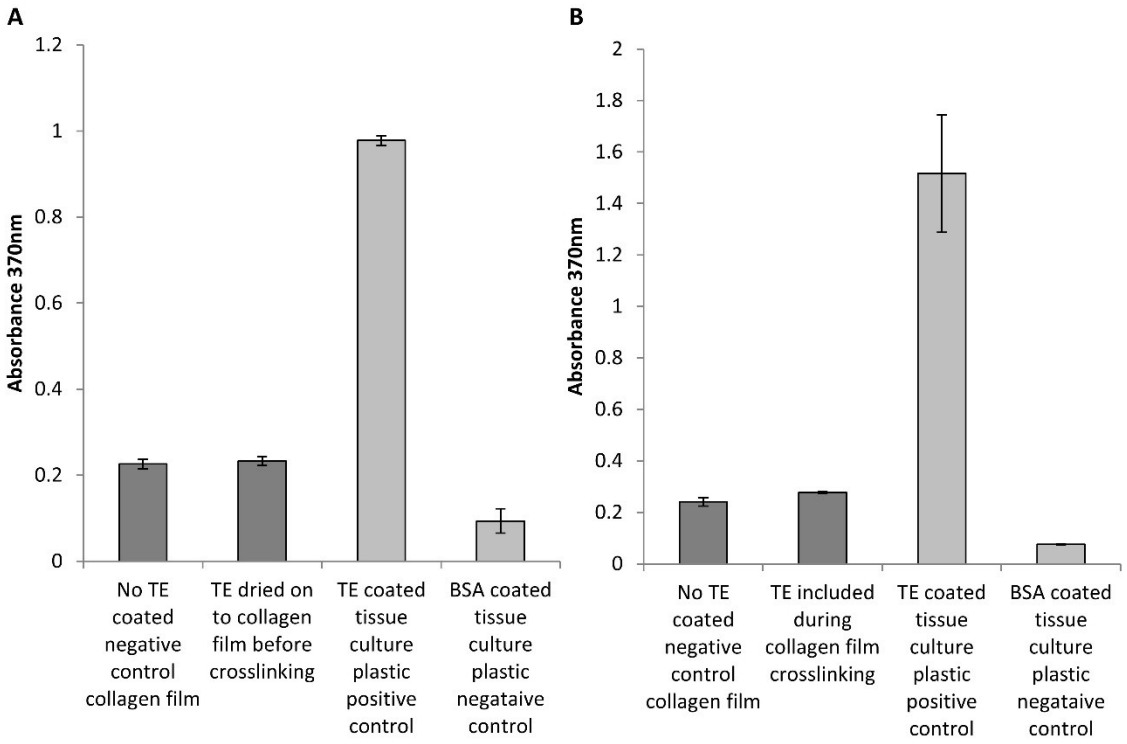

Supplementary figure 1 : BA-4 antibody ELISA detection of tropoelastin (TE) either dried onto collagen films from a 50 µg/mL tropoelastin solution prior to 100% EDC crosslinking (**A**) or included at 50 µg/mL tropoelastin during the 100% EDC crosslinking reaction (**B**). Negative control films, without tropoelastin coating, or bovine serum albumin (BSA) coated tissue culture plastic are shown. Tissue culture plastic coated with 50 µg/mL tropoelastin acts as a positive control. Error bars indicate S.D. of triplicate measurements.

Supplementary Figure 2

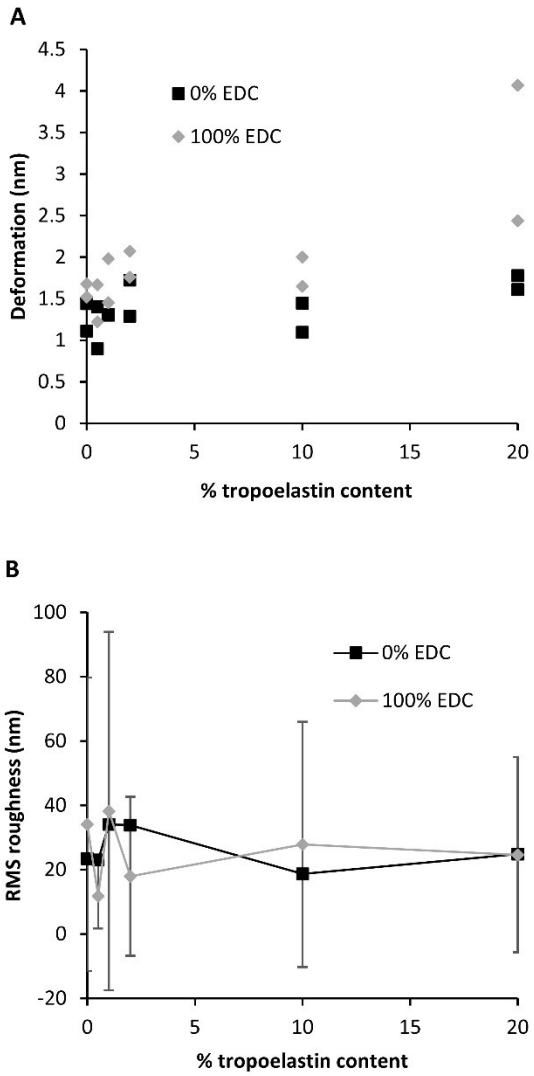

Supplementary figure 2 : QNM-derived deformation (**A**) or Root mean square (RMS) roughness (**B**) measurements of collagen films containing increasing tropoelastin (w/w) content. The films were either non-crosslinked or 100% EDC crosslinked. Error bars indicate S.D. of triplicates (**B**).

Supplementary Figure 3

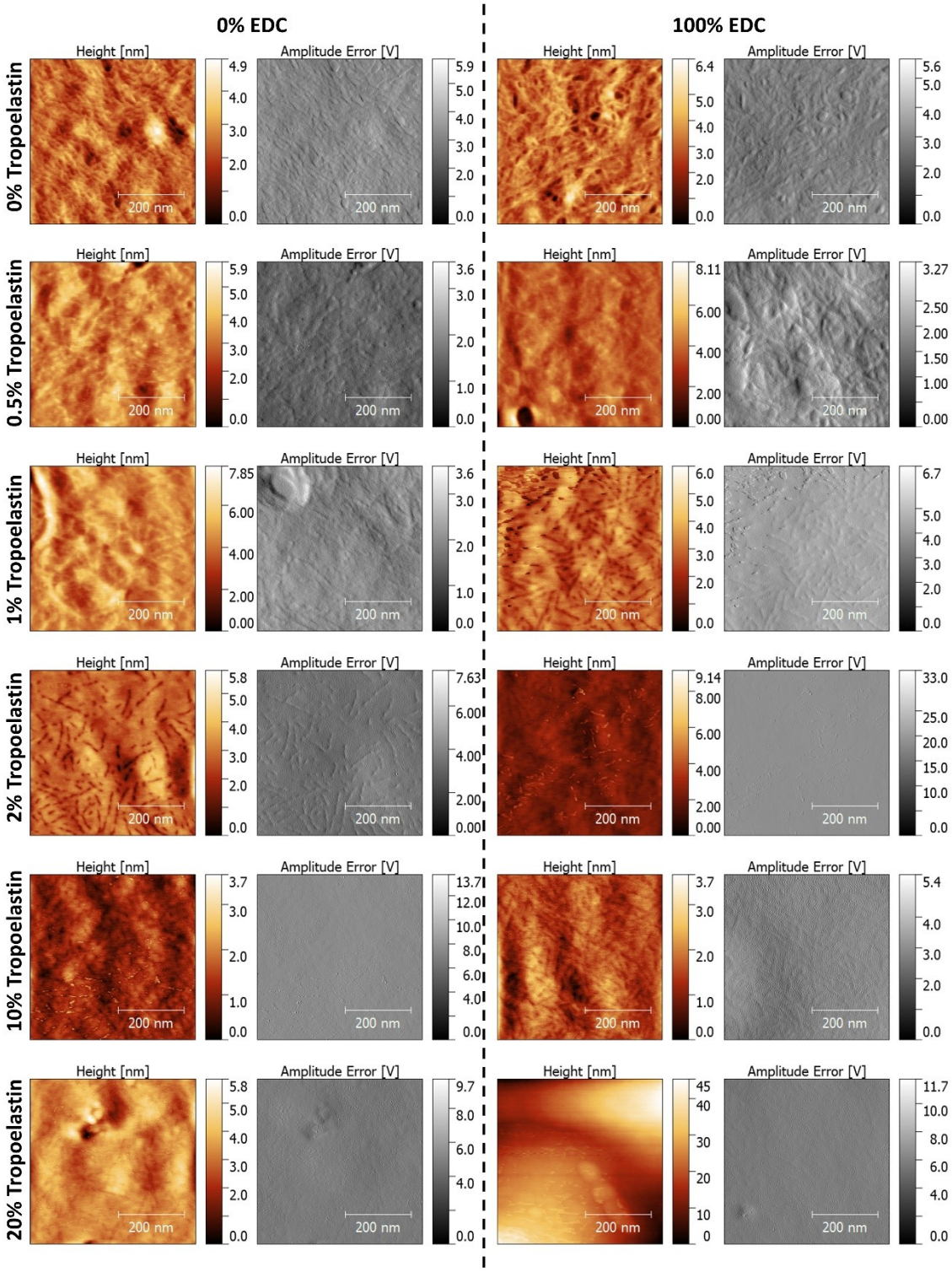

Supplementary figure 3 : Higher magnification (compared to figure 2) atomic force microscopy topographies of tropoelastin-collagen composite films containing increasing proportions of tropoelastin (expressed as % of total protein content). The films were either non-crosslinked or 100% EDC crosslinked. The scale bar indicates 200 nm.

Supplementary Figure 4

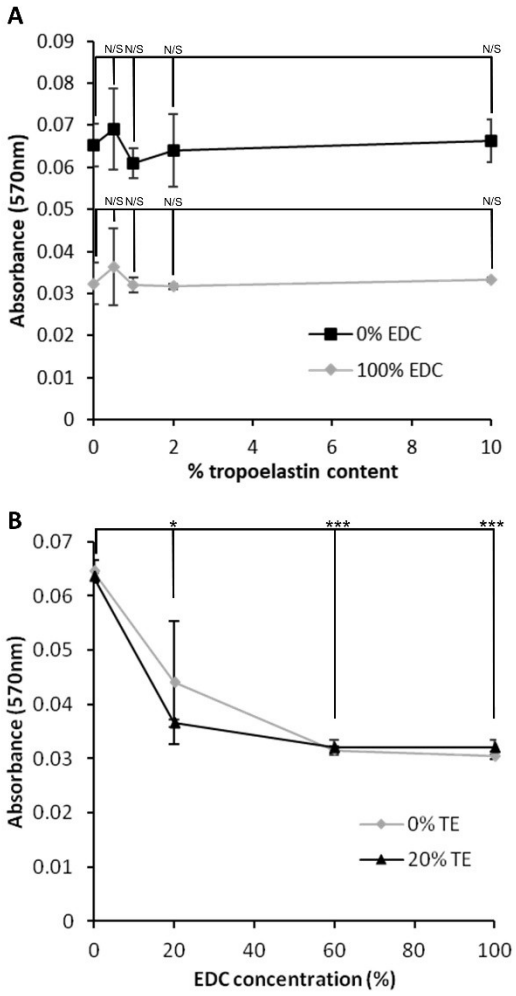

Supplementary figure 4 : Ninhydrin detection of free amine groups on collagen films containing increasing tropoelastin (w/w) content (**A**) or collagen-only films (0% TE) and collagen films containing 20% (w/w) tropoelastin (20% TE) crosslinked with increasing concentrations of EDC (**B**). For (**A**) the films were either non-crosslinked or 100% EDC crosslinked. Error bars indicate S.D. of triplicate measurements. Notation shows significance between the data points indicated.

Supplementary Figure 5

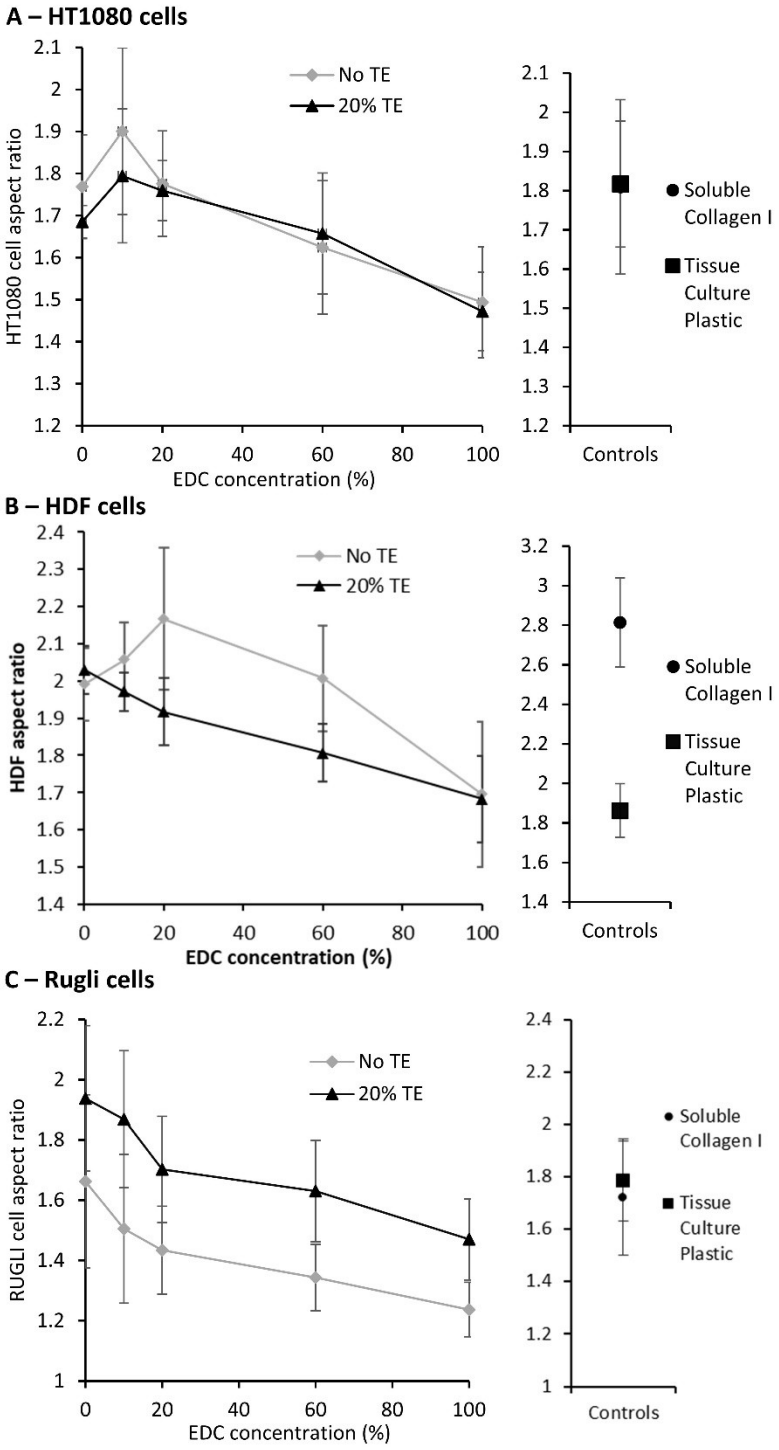

Supplementary figure 5 : Aspect ratio of HT1080 (**A**), human dermal fibroblasts (HDF – **B**) or Rugli cells (**C**) spreading onto collagen-only (No TE) or 20% tropoelastin-containing (20% TE) films crosslinked with increasing concentrations of EDC. Tissue culture plastic and 5 µg/mL collagen I controls are shown separately. Error bars indicate S.D. of six replicates.

Supplementary Figure 6A

Supplementary figure 6 : Rhodamine-phalloidin (actin assembly; orange) and DAPI (cell nuclei; light blue) fluorescent microscopy of HT1080 after 3 days in culture (**A**), human dermal fibroblasts after 3 days in culture (**B**), or Rugli cells after 3 and 5 days in culture (**C, D** respectively). Cells were cultured on collagen-only or 20% w/w tropoelastin-containing films crosslinked with increasing concentrations of EDC. Control images on tissue culture plastic (TCP) and 5 µg/mL soluble collagen I (Sol CN) are shown separately. Scale bar indicates 100 µm

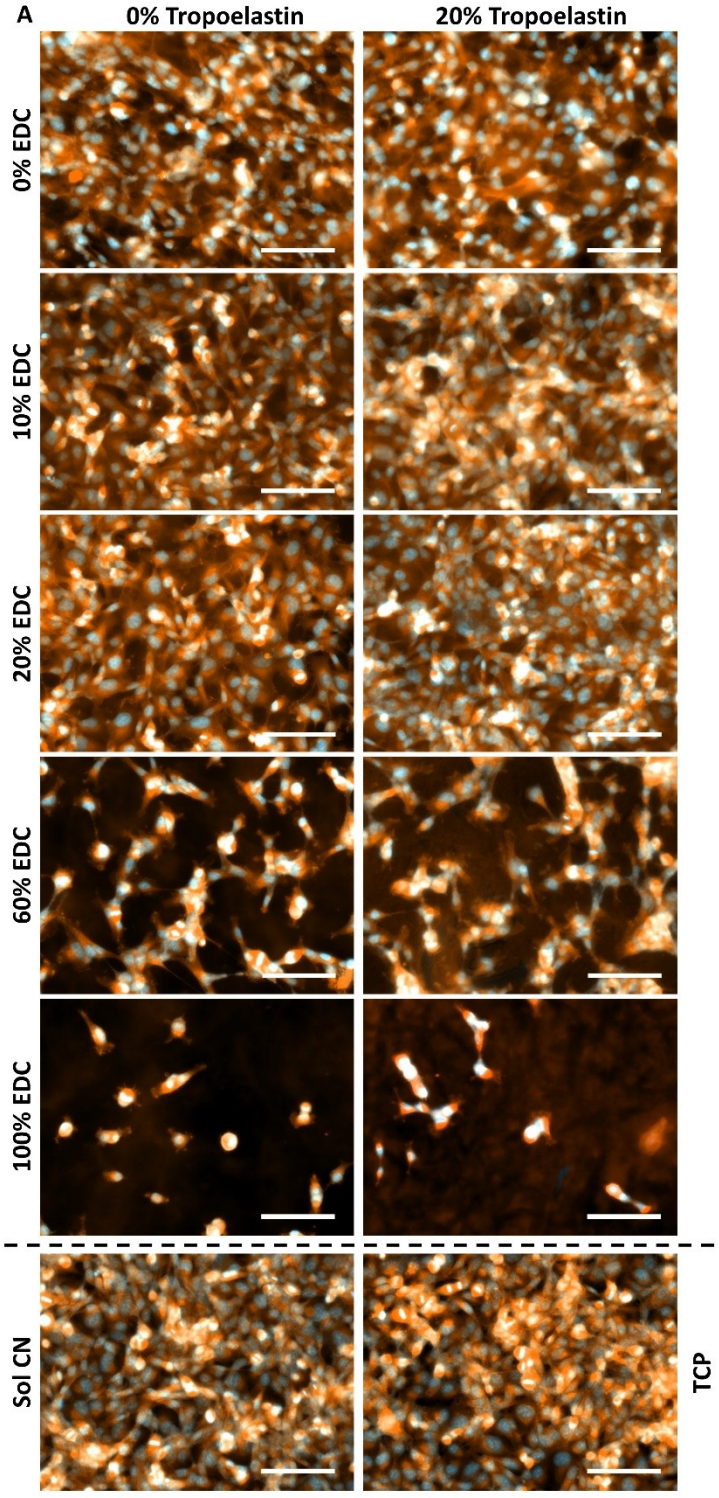

Supplementary Figure 6B

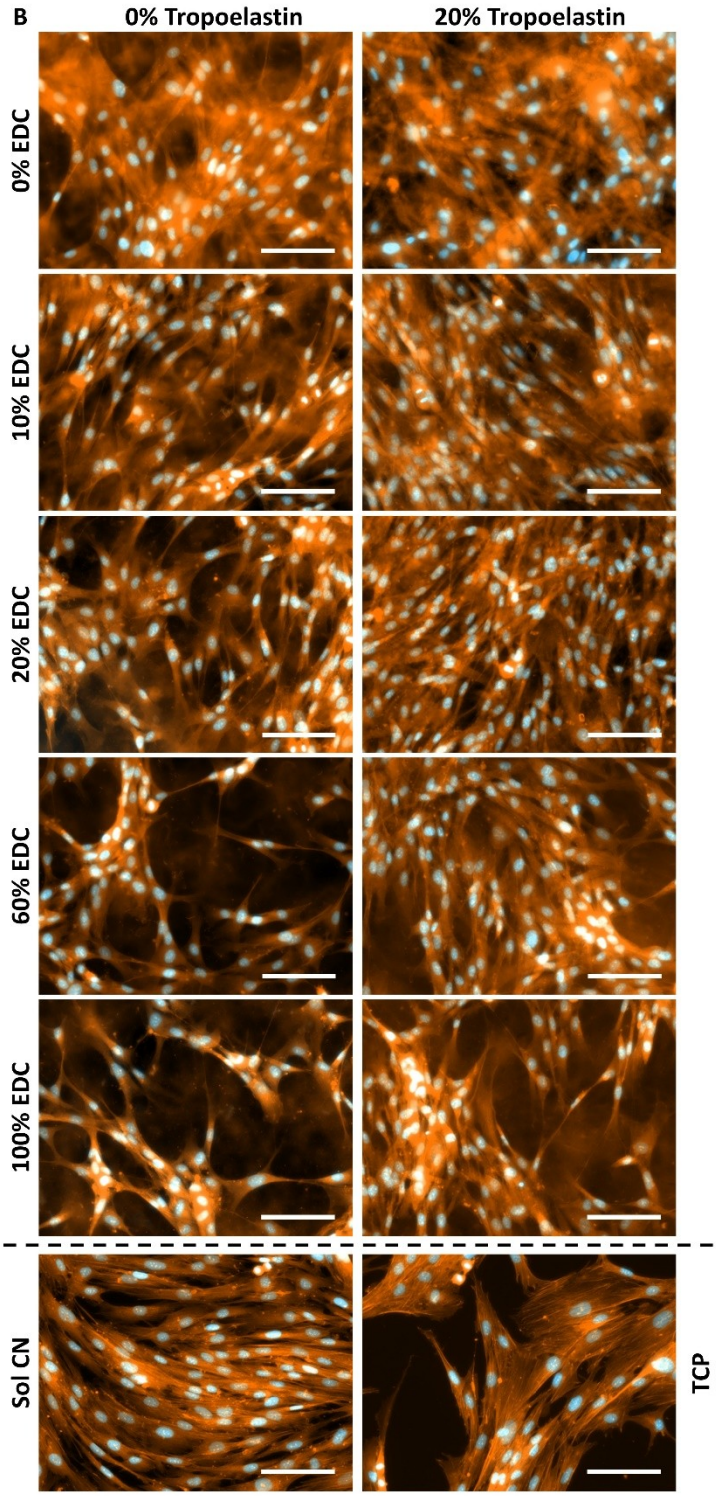

Supplementary Figure 6C

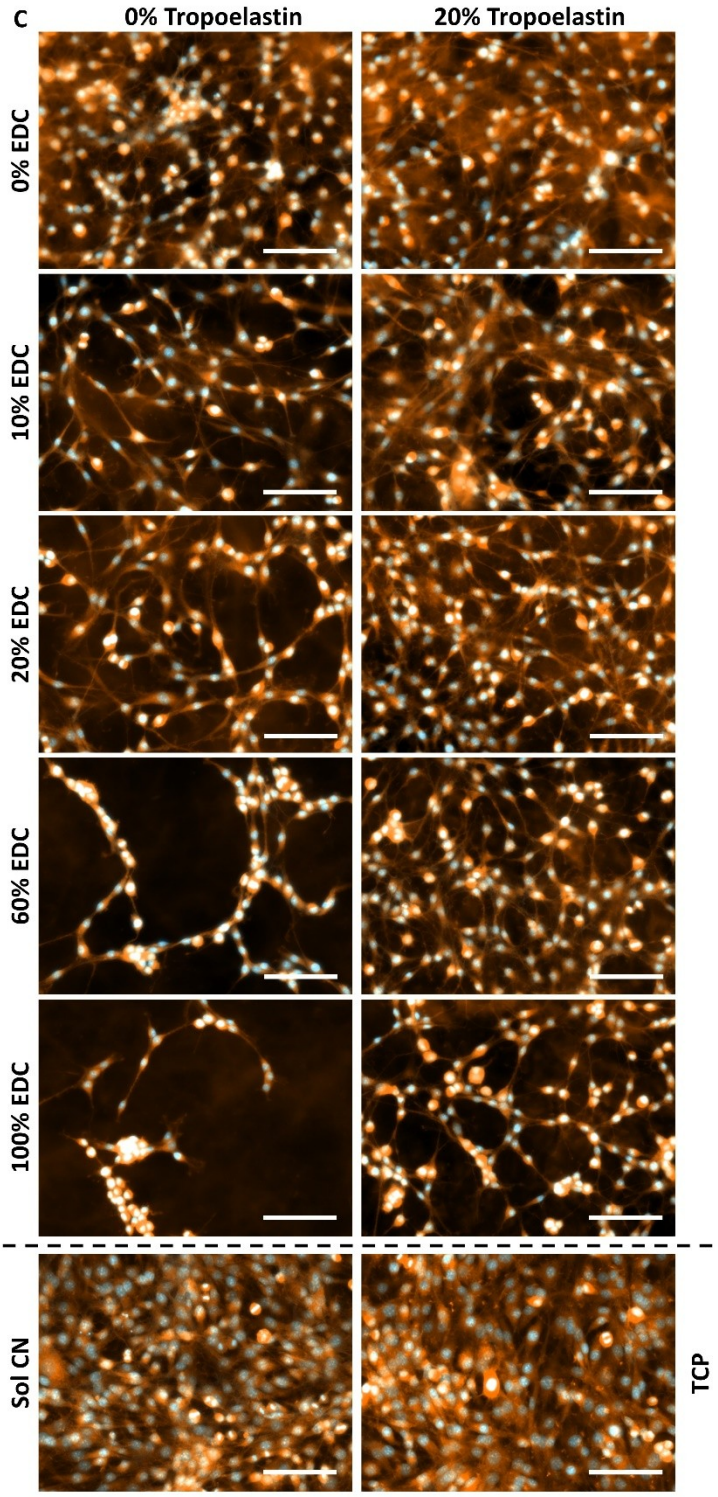

Supplementary Figure 6D